

On the Optimization and Stability of Sectorized Wireless Networks

Panagiotis Promponas, Tingjun Chen, and Leandros Tassioulas

Abstract—Future wireless networks need to support the increasing demands for high data rates and improved coverage. One promising solution is sectorization, where an infrastructure node is equipped with multiple sectors employing directional communication. Although the concept of sectorization is not new, it is critical to fully understand the potential of sectorized networks, such as the rate gain achieved when multiple sectors can be simultaneously activated. In this paper, we focus on sectorized wireless networks, where sectorized infrastructure nodes with beam-steering capabilities form a multi-hop mesh network. We present a sectorized node model and characterize the capacity region of these sectorized networks. We define the flow extension ratio and the corresponding sectorization gain, which quantitatively measure the performance gain introduced by node sectorization as a function of the network flow. Our objective is to find the sectorization of each node that achieves the maximum flow extension ratio, and thus the sectorization gain. Towards this goal, we formulate the corresponding optimization problem and develop an efficient distributed algorithm that obtains the node sectorization under a given network flow with an approximation ratio of $2/3$. Additionally, we emphasize the class of Even Homogeneous Sectorizations, which simultaneously enhances the efficiency of dynamic routing schemes with unknown arrival rates and increases network capacity. We further propose that if sectorization can be adapted dynamically over time, either a backpressure-driven or maximum weighted b-matching-based routing approach can be employed, thereby expanding the achievable capacity region while preserving stability under unknown traffic conditions. Through extensive simulations, we evaluate the sectorization gain and the performance of the proposed algorithms in various network scenarios.

Index Terms—Sectorized wireless networks, scheduling and routing, optimization

I. INTRODUCTION

Future wireless networks and systems including 5G/6G need to provide multi-Gbps data rates with guaranteed coverage, leveraging massive antenna systems [2], the widely available spectrum at millimeter-wave (mmWave) frequency [3], [4], and network densification [5]. In addition to deploying more cell sites, the *sectorization* of each cell – dividing each cell into a number of non-overlapping sectors – can significantly enhance the cell capacity and coverage by improving the spatial reuse and reducing interference [6].

There are many applications of sectorized networks to wireless access and backhaul networks, in both sub-6 GHz

and mmWave frequency bands. For example, in a mmWave backhaul network that can provide fiber-like data rates (e.g., the Terragraph 60 GHz solution [7]), each mmWave node is usually composed of a number of sectors, each of which is equipped with a phased array with beamforming capability [8], [9], [10]. In addition, integrated access and backhaul (IAB) [11] in the mmWave band supporting flexible and sectorized multi-hop backhauling started to be standardized since 3GPP Release 16. Recent efforts also focused on using increased number of sectors per infrastructure node to provide better coverage (e.g., SuperCell [12] supports 36 azimuth sectors per node). Therefore, it is important to study the performance of sectorized networks, especially when each node can simultaneously activate multiple sectors for signal transmission and/or reception.

In this paper, we focus on the *modeling, analysis, and optimization of sectorized wireless networks*, where sectorized nodes form a multi-hop mesh network for data forwarding and routing. In particular, we consider the scenario where a sectorized infrastructure node can simultaneously activate many sectors supporting beam-steering capability, and focus on optimizing the sectorization of each node given the network conditions. We present the model of a sectorized wireless backhaul network consisting of a number of (fixed) sectorized infrastructure nodes, and describe the link interference model and characterize the capacity region of these networks. For a sectorized network, we introduce a latent structure of its connectivity graph, called the auxiliary graph, which captures the underlying structural property of the network as a function of the sectorization of each node. We show that the capacity region of a sectorized network can be described by the matching polytope of its auxiliary graph.

Then, we present the definitions of *flow extension ratio* and the corresponding *sectorization gain* as a function of the network flow. These two metrics quantitatively measure how much the network flow can be extended in a sectorized wireless network, and thus quantifies the performance of the network sectorization. We formulate an optimization problem with the objective to find the optimal sectorization of the network that maximizes the flow extension ratio (i.e., achieves the highest sectorization gain) under a given network flow. Due to the analytical intractability of the problem, we develop a novel distributed algorithm, *SECTORIZE- n* , that approximates the optimal sectorization of each node in the network. We also prove that *SECTORIZE- n* is a $2/3$ -approximation algorithm.

Moreover, we motivate the sectorization of a network as a medium to embed a useful structural property in the network's “effective” topology. In particular, the sectorization choice changes the topology of the auxiliary graph, on which we can run the algorithms to study and operate the (sectorized)

This work was supported in part by NSF grants CNS-2128530, CNS-2128638, CNS-2146838, CNS-2211944, AST-2232458, ECCS-2434131, and by ARO MURI grant W911NF2110325. A partial and preliminary version of this paper appeared in ACM MobiHoc’23, Oct. 2023 [1].

P. Promponas and L. Tassioulas are with the Department of Electrical and Computer Engineering, Yale University, New Haven, CT, USA (email: {panagiotis.promponas, leandros.tassioulas}@yale.edu).

T. Chen is with the Department of Electrical and Computer Engineering, Duke University, Durham, NC, USA (email: tingjun.chen@duke.edu).

network. As a motivating example, we introduce a specific sectorization option, called Even Homogeneous Sectorization, which forces the Auxiliary Graph to be bipartite. Such a sectorization option both (i) simplifies the characterization of the capacity region, and (ii) speeds up the stabilization of the network under the backpressure dynamic policy even compared to the unsectorized network. Surprisingly, with sufficient distributed computing power, the more we sectorize the network, the more we increase its capacity region while we decrease the time needed for its stabilization.

While most existing research has focused on a single, fixed sectorization, recent technology advances might offer the prospect of dynamic sectorization, where nodes can continuously adjust their sector alignments. We also propose two complementary solutions that capitalize on this flexibility. First, a backpressure-driven heuristic that obtains an instantaneous flow estimate and then re-sectorizes to optimize performance with respect to that flow. Second, a throughput-optimal policy that jointly optimizes routing, scheduling, and sectorization via a maximum weighted b-matching formulation.

Finally, we numerically evaluate the performance of the proposed algorithm through extensive simulations. We consider both an example 7-node network and a large number of random networks with varying numbers of sectors per node, node density, and network flows. The simulation results confirm our analysis and show that the approximate sectorization gain increases sublinearly with respect to the number of sectors per infrastructure node. Moreover, the results show that the dynamic sectorization routing schemes can significantly expand the network's capacity region and unlock new performance gains not achievable with static sectorization.

To summarize, the main contributions of this paper include:

- (i) A general sectorized multi-hop wireless network model and a comprehensive characterization of its capacity region based on matching polytopes,
- (ii) A distributed approximation algorithm that optimizes the sectorization of each node under a given network flow with performance guarantee,
- (iii) A specific sectorization, called Even Homogeneous Sectorization, which simplifies the characterization of the capacity region, speeds up the stabilization of the network under the backpressure dynamic policy and increases the capacity.
- (iv) *Dynamic Sectorization Approaches*. We further extend our framework beyond a single fixed sectorization to a dynamic scenario, proposing both an efficient *backpressure-based heuristic* for real-time sector reconfiguration and a *throughput-optimal* solution leveraging maximum weighted b-matching.
- (v) Extensive simulations for performance evaluation of the proposed sectorized network model and algorithm.

We also note that the developed sectorized network model and analysis are general and applicable to other networks that share similar structures of the connectivity and auxiliary graphs.

The remainder of the paper is organized as follows: In Section II we discuss related work. Section III introduces the

system model, interference assumptions and preliminaries. In Section IV, we define the auxiliary graph and demonstrate how feasible schedules of sectorized networks correspond to its matchings. Section V presents our sectorization metrics, including flow extension ratio and sectorization gain. Section VI formulates the sectorization optimization and proposes a distributed approximation algorithm for the case of one-shot optimization decision. We then show in Section VII how a special class of sectorization can induce bipartite auxiliary graphs, simplifying the analysis and accelerating stabilization. Section VIII discusses extensions to dynamic sectorization, including heuristic and throughput optimal routing approaches. Section IX evaluates the proposed algorithms, Section X explores future directions and Section XI concludes the paper.

II. RELATED WORK

There has been extensive work on characterizing the capacity region of sub-6GHz wireless networks where each node is equipped with a single directional antenna (i.e., *without sectorization*), as well as on developing medium access control (MAC), scheduling, and routing algorithms for these directional networks [13], [14], [15]. Recently work also focused on mmWave networks where nodes apply beamforming techniques for directional communication, and considered multi-user MIMO and joint transmission [16], IAB [11], joint scheduling and congestion control [17], and the corresponding scheduling/routing and resource allocation problems in these networks. For networks *with sectorization*, recent work has considered the design of routing protocols when only a single sector can be activated at any time for each node (e.g., [18]).

Most relevant to our work are [19], [20], [21]. In particular, [19] focuses on efficient message broadcasting in multi-hop sectorized wireless networks, where each node has a pre-fixed sectorization. In [20] the authors consider the multi-hop link scheduling problem in self-backhauled mmWave cellular networks and applied deep reinforcement learning for minimizing the end-to-end delay. Moreover, [21] considers the relay optimization problem between macro and micro base stations in mmWave backhaul networks with at most two-hop path lengths. In contrast, our work uniquely focuses on (i) characterizing the fundamental capacity of sectorized wireless networks when multiple sectors can be simultaneously activated at each node, (ii) optimizing the node sectorization in these networks under different network flow conditions, and (iii) analyzing the network-level gain introduced by optimizing the sectorization of each node, which has not been considered in prior work. To the best of our knowledge, this paper is *the first thorough study of these topics*.

III. MODEL AND PRELIMINARIES

In this section, we present the sectorized network model and the corresponding interference constraints and capacity region.

A. Network Model

We consider a network consisting of N *sectorized* infrastructure nodes. We denote the set of nodes by \mathcal{N} and index them by $[n] = \{1, 2, \dots, N\}$. In particular, let σ_n denote the

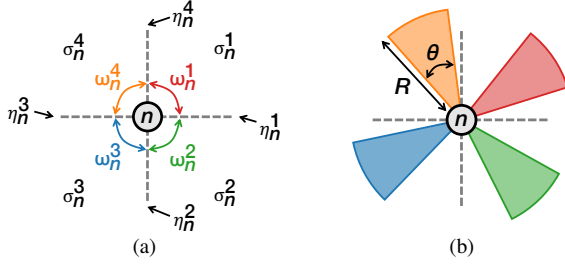


Fig. 1: Sectorized infrastructure node model: (a) A sectorized node n with $K_n = 4$ sectors, $\{\sigma_n^k\}$, the corresponding field of view (FoV) of each sector, $\{\omega_n^k\}$, and the sectoring axes, $\{\eta_n^k\}$. (b) Each node sector can perform transmit (TX) or receive (RX) beamforming with a range of R and main lobe beamwidth of θ .

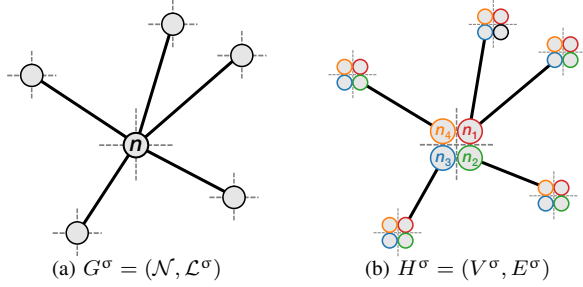


Fig. 2: Graph representations of a sectorized network: (a) the connectivity graph of the physical network, $G^\sigma = (\mathcal{N}, \mathcal{L}^\sigma)$, and (b) its corresponding auxiliary graph, $H^\sigma = (V^\sigma, E^\sigma)$.

sectorization of node $n \in \mathcal{N}$ equipped with K_n sectors. Let $\Gamma_n(K_n)$ denote the set of all possible sectorizations for node n with a fixed number of K_n sectors. As shown in Fig. 1(a), the k^{th} sector of node n , denoted by σ_n^k ($k = 1, \dots, K_n$), has a field of view¹ (FoV) of ω_n^k , and the K_n sectors of node n combine to cover an FoV of the entire azimuth plane, i.e., $\sum_{k=1}^{K_n} \omega_n^k = 360^\circ$. For two adjacent sectors k and $(k+1)$ of node n ($k = 1, \dots, K-1$), we call their boundary a *sectoring axis* and denote it by η_n^k . We define the sectoring axis between sector K and sector 1 with η_n^K . Let $\sigma = (\sigma_1, \dots, \sigma_N) = [\sigma_n : \forall n \in \mathcal{N}]$ denote the *network sectorization*, and $\mathbf{K} = (K_1, \dots, K_N) = [K_n : \forall n \in \mathcal{N}]$ be the vector of the number of sectors for all nodes. For a given $\mathbf{K} \in \mathbb{Z}_+^N$, let $\Gamma(\mathbf{K})$ be the set of all possible network sectorizations, where node n is equipped with K_n sectors.

Each sector of an infrastructure node is equipped with a half-duplex phased array antenna to perform transmit (TX) or receive (RX) beamforming. We adapt the sectorized antenna model [22] to approximate the TX/RX beam pattern that can be formed by each sector, where R is the TX/RX range and θ is the beamwidth of the main lobe, as depicted in Fig. 1(b). We assume that the beamwidth θ is smaller than the sector's FoV, and the TX/RX beam can be *steered* to be pointed in different directions within each sector.

We use a *directed* graph $G^\sigma = (\mathcal{N}, \mathcal{L})$ to denote the *connectivity graph* of the network under sectorization $\sigma \in \Gamma(\mathbf{K})$, where \mathcal{N} (with $|\mathcal{N}| = N$) is the set of nodes and \mathcal{L} (with $|\mathcal{L}| = L$) is the set of directed links. A directed link ℓ from

node n to node n' , denoted by $\ell = (n, n')$, exists if the distance between the two nodes is less than the sum of their communication range, i.e., $|\mathbf{x}(n) - \mathbf{x}(n')| \leq 2R$, where $\mathbf{x}(x)$ denotes the node's location vector (e.g., using the Cartesian coordinate system) and $|\cdot|$ denotes the L_2 -norm. Without loss of generality, we use G (without the superscript σ) to denote the connectivity graph of an unsectorized network.

We also present an equivalent representation of each directed link in G^σ based on the node sectors. In particular, each $\ell \in \mathcal{L}$ can also be represented by $\ell = (\sigma_n^k, \sigma_{n'}^{k'})$, where the k^{th} sector of node n (i.e., σ_n^k) is the *TX sector*, and the k'^{th} sector of node n' (i.e., $\sigma_{n'}^{k'}$) is the *RX sector*. For a link in the form of $(\sigma_n^k, \sigma_{n'}^{k'})$ to be a *feasible* link, it needs to satisfy the following two conditions² (see Fig. 3(a)):

- **(C1)** The distance between the two nodes is less than the sum of their communication range, i.e., $|\mathbf{x}(n) - \mathbf{x}(n')| \leq 2R$; and
- **(C2)** Node n lies in the FoV $\omega_{n'}^{k'}$ of node n' , and node n' lies in the FoV ω_n^k of node n .

Since both the TX and RX beams can be steered within ω_n^k of node n and $\omega_{n'}^{k'}$ of node n' , respectively, the above two conditions are sufficient for establishing $\ell = (\sigma_n^k, \sigma_{n'}^{k'})$. Moreover, if $(\sigma_n^k, \sigma_{n'}^{k'})$ is a directional link, $(\sigma_{n'}^{k'}, \sigma_n^k)$ is also a directional link due to symmetry. Therefore, the set of feasible directed edges in G^σ is given by:

$$\begin{aligned} \mathcal{L} &= \{(n, n') : \forall n, n' \in \mathcal{N}, n \neq n', \text{ s.t. (C1) is satisfied}\}, \text{ or} \\ \mathcal{L}^\sigma &= \{(\sigma_n^k, \sigma_{n'}^{k'}) : \forall n, n' \in \mathcal{N}, n \neq n', k \in [K_n], k' \in [K_{n'}], \\ &\quad \text{s.t. (C1) and (C2) are satisfied}\}. \end{aligned}$$

Although \mathcal{L} and \mathcal{L}^σ are identical with respect to G^σ , for clarity, we use \mathcal{L}^σ with superscript σ to indicate the directed links represented by node sectors. Moreover, let $\mathcal{L}_n^+, \mathcal{L}_n^- \subseteq \mathcal{L}^\sigma$ denote the set of (directed) outgoing and incoming links with end point of node n .

Remark. Note that one of the main differences between the sectorized and traditional unsectorized networks is that *each node $n \in \mathcal{N}$ can have multiple links being activated at the same time, at most one per sector*. As a result, a number of links in \mathcal{L}^σ can share the same end point (node) in \mathcal{N} while being activated simultaneously. We use the terms “node” and “link” in reference to the *connectivity graph*, G^σ , while reserving the terms “vertex” and “edge” for the *auxiliary graph* of G^σ , which will be presented in Section IV.

B. Interference Model

The link interference model is essential for determining the set of directional links that can be activated simultaneously, or the *feasible schedules*. Below, we describe our link interference model based on the protocol model [24] adapted to the considered sectorized networks.

Definition 3.1 (Primary Interference Constraints in Sectorized Networks). *The transmission on a feasible link $(\sigma_n^k, \sigma_{n'}^{k'}) \in \mathcal{L}^\sigma$*

¹We define the field of view of a sector as the angular coverage in the azimuth plane that this sector can transmit to or receive from.

²A similar interference model was presented in [23], where beamforming can reduce the interference in mmWave networks. Our framework can also be generalized to other types of networks using their corresponding connectivity graphs.

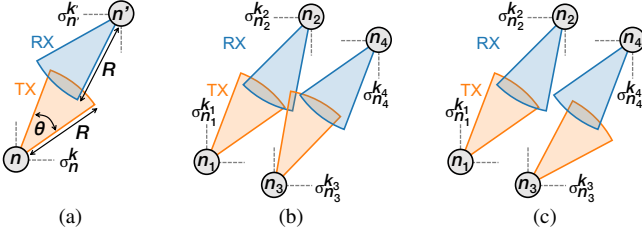


Fig. 3: (a) A feasible link $\ell = (\sigma_n^k, \sigma_{n'}^k)$, (b) A secondary interfering TX sector $\sigma_{n_3}^{k_3}$ to RX sector $\sigma_{n_2}^{k_2}$, (c) The secondary TX interference in (b) can be avoided by steering node 3's TX beam in $\sigma_{n_3}^{k_3}$, so that both links $(\sigma_{n_1}^{k_1}, \sigma_{n_2}^{k_2})$ and $(\sigma_{n_3}^{k_3}, \sigma_{n_4}^{k_4})$ can be simultaneously activated.

from the k^{th} sector of node n to the k'^{th} sector of node n' is successful if it does not overlap with any other feasible directional link (σ_n^k, σ_m^j) or $(\sigma_m^j, \sigma_{n'}^{k'})$ that share a TX or RX sector in common with $(\sigma_n^k, \sigma_{n'}^{k'})$. Essentially, at any time, at most one outgoing or incoming link is allowed in each node sector $\sigma_n^k, \forall n \in \mathcal{N}, k \in [K_n]$.

Definition 3.2 (Secondary Interference Constraints in Sectorized Networks). Consider two feasible directional links $\ell_{12} = (\sigma_{n_1}^{k_1}, \sigma_{n_2}^{k_2})$ and $\ell_{34} = (\sigma_{n_3}^{k_3}, \sigma_{n_4}^{k_4})$ between four distinct nodes n_i ($i = 1, 2, 3, 4$) with fixed beamforming directions in each TX/RX sector. If the directional link $\ell_{32} = (\sigma_{n_3}^{k_3}, \sigma_{n_2}^{k_2})$ is also a feasible link and the TX beam in $\sigma_{n_3}^{k_3}$, which is intended to communicate with the RX beam in $\sigma_{n_4}^{k_4}$, overlaps with the RX beam in $\sigma_{n_2}^{k_2}$, then $\sigma_{n_3}^{k_3}$ is a secondary interfering TX sector to the RX sector $\sigma_{n_2}^{k_2}$ (see Fig. 3(b)).

In this paper, we consider only primary interference constraints in sectorized networks, which is a realistic assumption because of two main reasons. First, note that secondary interference constraints can be avoided using the beam steering capacity of an infrastructure node. For the example depicted in Fig. 3(b), the interference from TX sector $\sigma_{n_3}^{k_3}$ to RX sector $\sigma_{n_2}^{k_2}$ can be avoided by steering the TX beam of node 3 in $\sigma_{n_3}^{k_3}$, so that both links $(\sigma_{n_1}^{k_1}, \sigma_{n_2}^{k_2})$ and $(\sigma_{n_3}^{k_3}, \sigma_{n_4}^{k_4})$ can be activated simultaneously, as shown in Fig. 3(c). Second, it is intuitive to note that for sufficiently small values of the beamwidth, θ , the network becomes highly directional with “pencil” beams. Essentially, there exists a threshold for θ , denoted by θ_{th} , below which the secondary interference constraints can be completely eliminated regardless of the TX/RX beamforming directions at each node. For each node n , let θ_n^{\min} denote the minimum angle between adjacent links with n being an endpoint. Then, we have $\theta_{\text{th}} = \min_{n \in \mathcal{N}} \{\theta_n^{\min}\}$. In the example network shown in Fig. 6 (see Section IX-A for the detailed setup), $\theta_{\text{th}} = 15.8^\circ$, which can be achieved by state-of-the-art phased arrays [8]. Fig. 4 illustrates the cumulative distribution function (CDF) of θ_{th} calculated over 1,000 random networks (see Section IX-B for the detailed setup) with $N \in \{20, 40, 60\}$ nodes deployed in a unit square area and when a communication range of $2R = 0.1$. The median value for θ_{th} is $107.0^\circ/6.7^\circ/2^\circ$ for $N = 20/40/60$, respectively. This illustrates that in certain scenarios, it is reasonable to remove the secondary interference constraint

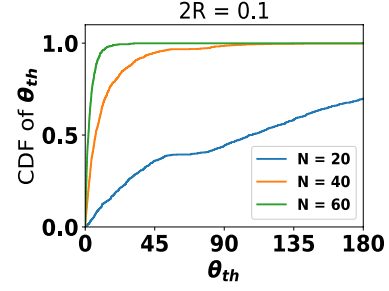


Fig. 4: The CDF of θ_{th} calculated for 1,000 random networks with $N \in \{20, 40, 60\}$ and a communication range of $2R = 0.1$.

under realistic node density and beamwidth. Note that a single sector can include multiple links, but at most one link can be activated in any time slot. Under our no-secondary-interference assumption, we assume the beam can be aligned with whichever link is scheduled within that sector.

C. Traffic Model, Schedule, and Queues

We assume that time is slotted and packets arrive at each node according to some stochastic process. For convenience, we classify all packets passing through the network to belong to a particular commodity, $c \in \mathcal{N}$, which represents the destination node of each packet. Let $A_n^{(c)}(t) \leq A_{\max} < +\infty$ be the number of commodity- c packets entering the network at node n and destined for node c in slot t . The packet arrival process $A_n^{(c)}(t)$ is assumed to have a well-defined long-term rate of $\alpha_n^{(c)} = \lim_{T \rightarrow +\infty} \frac{1}{T} \sum_{t=1}^T A_n^{(c)}(t)$. Let $\alpha = [\alpha_n^{(c)}]$ be the $N \times N$ multi-commodity arrival rate matrix.

All the (directional) links have a capacity of one packet per time slot³. A schedule in any time slot t is represented by a vector $\mathbf{X}(t) = [X_\ell(t)] \in \{0, 1\}^L$, in which $X_\ell(t) = 1$ if link ℓ is scheduled to transmit a packet in time slot t and $X_\ell(t) = 0$ otherwise. We denote the set of feasible schedules in G^σ by \mathcal{X}_{G^σ} . In addition, let $\mu_\ell^{(c)}(t) = 1$ if link ℓ serves a commodity- c packet in time t (determined by the scheduling and routing algorithm), and $\mu_\ell^{(c)}(t) = 0$ otherwise. We define $Q_n^{(c)}(t)$ as the number of commodity- c packets at node n in time slot t , or the queue backlog. Choosing a schedule $\mathbf{X}(t) \in \mathcal{X}_{G^\sigma}$ and let $[x]^+ = \max\{0, x\}$, the queue dynamics are described by:

$$Q_n^{(c)}(t) = [Q_n^{(c)}(t-1) - \sum_{\ell \in \mathcal{L}_n^+} X_\ell(t) \cdot \mu_\ell^{(c)}(t)]^+ + \sum_{\ell \in \mathcal{L}_n^-} X_\ell(t) \cdot \mu_\ell^{(c)}(t) + A_n^{(c)}(t), \forall t.$$

Let $\mathbf{Q}(t) = [Q_n^{(c)}(t) : n, c \in \mathcal{N}]$ denote the queue vector.

D. Capacity Region & Throughput Optimality

A dynamic scheduling and routing algorithm will determine the schedule $\mathbf{X}(t)$ in each time t . Let $f_\ell^{(c)}$ denote the long-term rate at which commodity- c packets are served by link ℓ , or the commodity- c flow on link ℓ . We define $\mathbf{f} = [f_\ell : \ell \in \mathcal{L}^\sigma]$ as the network flow vector, where $f_\ell = \sum_{c \in \mathcal{N}} f_\ell^{(c)}$ is the total

³For simplicity, our analysis uses unit-capacity links, but we expect the same framework to extend to heterogeneous capacities by applying each link's capacity as a multiplicative factor in both the feasible flow region and the max-weight scheduling (cf. [25, Section 4.3]).

flow served by link ℓ . The capacity region of the considered sectorized network G^σ , denoted by $\Lambda(G^\sigma)$, is defined as the set of all arrival rate matrices, α , for which there exists a multi-commodity network flow vector, \mathbf{f} , satisfying the flow conservation equations given by:

$$\alpha_{nc} = \sum_{\ell \in \mathcal{L}_n^+} f_\ell^{(c)} - \sum_{\ell \in \mathcal{L}_n^-} f_\ell^{(c)}, \quad \forall n \in \mathcal{N} \text{ and } n \neq c, \quad (1)$$

$$\sum_{n \in \mathcal{N}} \alpha_{nc} = \sum_{\ell \in \mathcal{L}_c^-} f_\ell^{(c)}, \quad \forall c \in \mathcal{N}, \quad (2)$$

$$f_\ell^{(c)} \geq 0, \quad \forall \ell \in \mathcal{L}^\sigma, c \in \mathcal{N}, \quad (3)$$

$$f_\ell = \sum_{c \in \mathcal{N}} f_\ell^{(c)} \leq 1, \quad \forall \ell \in \mathcal{L}^\sigma. \quad (4)$$

In particular, (1)–(3) define a *feasible* routing for commodity- c packets, and (4) indicates that the total flow on each edge should not exceed its capacity. Therefore, for $G^\sigma = (\mathcal{N}, \mathcal{L}^\sigma)$, an arrival rate matrix α is in the capacity region $\Lambda(G^\sigma)$ if there exists a *feasible* multi-commodity flow vector supporting α with respect to the network defined by G^σ . As a result,

$$\Lambda(G^\sigma) = \left\{ \alpha : \exists \mathbf{f} \in \text{Co}(\mathcal{X}_{G^\sigma}) \text{ s.t. (1)–(4) are satisfied} \right\}, \quad (5)$$

where $\text{Co}(\cdot)$ is the convex hull operator.

A scheduling and routing algorithm is called *throughput-optimal* if it can keep the network queues stable for all arrival rate matrices $\alpha \in \text{int}(\Lambda(G^\sigma))$, where $\text{int}(\Lambda(G^\sigma))$ denotes the interior of $\Lambda(G^\sigma)$. A well-known throughput-optimal algorithm is the dynamic *backpressure routing algorithm* [26], which works as follows. For each link $\ell = (n, m) \in \mathcal{L}^\sigma$, we define its *backpressure* in time slot t as $D_\ell(t) = \max_{c \in \mathcal{N}} \{Q_n^{(c)}(t) - Q_m^{(c)}(t)\}$. Let $\mathbf{D}(t) = [D_\ell(t) : \forall \ell \in \mathcal{L}^\sigma]$. In every time slot t , the backpressure algorithm selects $\mathbf{X}^{\text{BP}}(t)$ as follows:

$$\mathbf{X}^{\text{BP}}(t) \in \arg \max_{\mathbf{X} \in \mathcal{X}_{G^\sigma}} \{\mathbf{D}^\top(t) \cdot \mathbf{X}\}, \quad (6)$$

together with the commodity to be served on each link ℓ . Given $\alpha \in \text{int}(\Lambda(G^\sigma))$, the backpressure algorithm returns a feasible network flow \mathbf{f} that supports α in G^σ . In the rest of the paper, although the target optimization problems may admit multiple optimal solutions, without loss of generality and for notational brevity, we treat them as singletons.

IV. THE AUXILIARY GRAPH AND MATCHINGS

In this section, we introduce the auxiliary graph for a sectorized network, followed by an overview of matching polytopes and the definition of equivalent sectorizations. All of these serve as the foundations for the results presented in the remaining of this paper.

A. The Auxiliary Graph, H^σ

To allow for analytical tractability and support the analysis, we introduce the *auxiliary graph*, $H^\sigma = (V^\sigma, E^\sigma)$ of the considered sectorized network, under a given sectorization rule, $\sigma \in \Gamma(\mathbf{K})$. In particular, H^σ is generated based on the connectivity graph $G^\sigma = (\mathcal{N}, \mathcal{L}^\sigma)$ as follows:

- Each node $n \in V$ is duplicated K_n times into a set of *vertices*, $\{n_1, \dots, n_{K_n}\} \in V^\sigma$, one for each node sector σ_n^k , $k \in [K_n]$.
- Each directed link $\ell = (\sigma_n^k, \sigma_{n'}^{k'}) \in \mathcal{L}^\sigma$ between the TX sector σ_n^k and RX sector $\sigma_{n'}^{k'}$ is “inherited” as a directed *edge* e from vertex n_k to vertex $n'_{k'}$ in V^σ .

Note that $|V^\sigma| = \sum_{n \in \mathcal{N}} K_n$ and $|E^\sigma| = |\mathcal{L}| = L$, and as we show in the rest of the paper, H^σ can facilitate the analysis and optimization in sectorized networks. An illustrative example is shown in Fig. 2, where each node in G^σ has an equal number of 4 sectors based on the Cartesian coordinate system. Node n in G^σ is duplicated 4 times to become n_i ($i = 1, 2, 3, 4$) in H^σ , while the 5 feasible links in \mathcal{L}^σ are “inherited” from G^σ to H^σ , whose end points are the duplicated vertices representing the corresponding TX/RX sectors.

B. Feasible Schedules in G^σ as Matchings in H^σ

For an unsectorized network G (i.e., $\sigma = \emptyset$) with $K_n = 1, \forall n$, its auxiliary graph $H = (V, E)$ is identical to the connectivity graph $G = (\mathcal{N}, \mathcal{L})$. Therefore, we use G and H interchangeably when referring to an unsectorized network. Each feasible schedule $\mathbf{X} \in \mathcal{X}_G$ is a *matching* – a set of links among which no two links share a common node – in G (and thus in H).

In a sectorized network $G^\sigma = (\mathcal{N}, \mathcal{L}^\sigma)$, a feasible schedule in G^σ may not be a matching in G^σ , since up to K_n links can share a common node n . However, under the primary interference constraints and with the use of the auxiliary graph, *any* feasible schedule in G^σ corresponds to a matching in H^σ . Let $\mathbf{M} \in \{0, 1\}^L$ denote a matching vector in H^σ , in which every element (edge) is ordered according to the position of the element (link) that it corresponds to in \mathbf{X} . Let \mathcal{M}_{H^σ} be the set of matchings in H^σ . To rigorously connect a feasible schedule $\mathbf{X} \in \mathcal{X}_{G^\sigma}$ in G^σ to a matching $\mathbf{M} \in \mathcal{M}_{H^\sigma}$ in H^σ , we need to take a deeper look into the sets \mathcal{L}^σ and E^σ : they not only have the same cardinality of L , but are also in fact two *isomorphic* sets. Due to the way H^σ is constructed, there exists an isomorphism $\mathcal{O} : E^\sigma \rightarrow \mathcal{L}^\sigma$ such that for $e = (n_k, n'_{k'}) \in E^\sigma$ and $\ell = (\sigma_n^k, \sigma_{n'}^{k'}) \in \mathcal{L}^\sigma$, $\mathcal{O}(e) = \ell$.

C. Background on Matching Polytopes

The *matching polytope* of a (general) graph $G = (V, E)$, denoted by \mathcal{P}_G , is a convex polytope whose corners correspond to the matchings in G , and can be described using Edmonds’ matching polytope theorem [27]. Specifically, a vector $\mathbf{x} = [x_e : e \in E] \in \mathbb{R}^{|E|}$ belongs to \mathcal{P}_G if and only if it satisfies the following conditions [27], [28]:

- (P) (i) $x_e \geq 0, \forall e \in E$, and $\sum_{e \in \delta(v)} x_e \leq 1, \forall v \in V$,
(ii) $\sum_{e \in E(U)} x_e \leq \lfloor |U|/2 \rfloor, \forall U \subseteq V$ with $|U|$ odd, (7)

where $\delta(v)$ is the set of edges incident to v , and $E(U)$ is the set of edges in the subgraph induced by $U \subseteq G$. Note that in general, it is challenging to compute \mathcal{P}_G , since (ii) of (7) includes an exponential number of constraints since all sets of vertices $U \subseteq V$ with an odd cardinality need to be enumerated

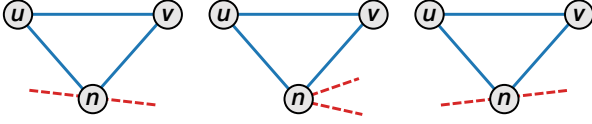


Fig. 5: Three equivalent sectorizations for a node $n \in \mathcal{N}$.

through. The *fractional matching polytope* of G , denoted by \mathcal{Q}_G , is given by

$$(Q) \quad x_e \geq 0, \forall e \in E, \text{ and } \sum_{e \in \delta(v)} x_e \leq 1, \forall v \in V. \quad (8)$$

For a general graph G , $\mathcal{P}_G \subseteq \mathcal{Q}_G$ since (ii) in (P) is excluded in (Q). For a bipartite graph G_{bi} ⁴, its matching polytope and fractional matching polytope are equivalent, i.e., $\mathcal{P}_{G_{bi}} = \mathcal{Q}_{G_{bi}}$ [29].

Recall that for an unsectorized network G , its auxiliary graph $H \equiv G$ and its matching polytope is the convex hull of the set of matchings, i.e., $\mathcal{P}_H = \text{Co}(\mathcal{M}_H)$. Therefore, its capacity region $\Lambda(G)$ is determined by \mathcal{P}_H , since $\mathcal{X}_G = \mathcal{M}_H$. For a sectorized network G^σ , since a feasible schedule in G^σ , $\mathbf{X} \in \mathcal{X}_{G^\sigma}$, corresponds to a matching in the auxiliary graph H^σ , $\mathbf{M} \in \mathcal{M}_{H^\sigma}$ (see Section IV-B), we show in Section V that its capacity region, $\Lambda(G^\sigma)$, can be determined by the matching polytope of H^σ , \mathcal{P}_{H^σ} (Lemma 1).

D. Equivalent Sectorizations

Since our objective is to obtain the optimal sectorization for each node in the network, it is important to understand the structural property of a sectorization, σ . In particular, for a node $n \in \mathcal{N}$ with K_n number of sectors, there is only a *finite number of distinct sectorizations* in $\Gamma_n(K_n)$, due to the equivalent classes of sectorizations.

Consider a node $n \in \mathcal{N}$ and two of its undirected adjacent incident links $\ell_1 = (n, u)$ and $\ell_2 = (n, v)$ for some u, v incident to n . To define the undirected links from the set \mathcal{L} , we assume, for example, that the undirected link ℓ_1 includes the two directed links $(n, u) \in \mathcal{L}_n^+$ and $(u, n) \in \mathcal{L}_n^-$. Note that, under the primary interference constraints, it does not make a difference where exactly a sectorization axis is put between ℓ_1 and ℓ_2 of node n . What matters is whether a sectorization axis will be placed between them or not. If two sectorizations $\sigma_1 \in \Gamma_n(K_n)$ and $\sigma_2 \in \Gamma_n(K_n)$ differ only on the exact position of a sectorization axis while both sectorization have a sectoring axis placed between ℓ_1 and ℓ_2 , it holds that $H^{\sigma_1} \equiv H^{\sigma_2}$, and thus $\mathcal{M}_{H^{\sigma_1}} = \mathcal{M}_{H^{\sigma_2}}$. Hence, the set $\Gamma_n(K_n)$ consists of a finite number of equivalent sectorizations.

Fig. 5 depicts an example of three equivalent sectorizations for node n , where both links $\ell_1 = (n, u)$ and $\ell_2 = (n, v)$ are placed within the same sector. Note that this notion of equivalent sectorizations makes the optimization over the set $\Gamma(\mathbf{K})$, for every fixed $\mathbf{K} \in \mathbb{Z}_+^N$, more approachable. Motivated by the comparison of sectorizations of Fig. 5, when rotating a sectorization axis of node n , an infinite number of

equivalent sectorizations can be generated until the axis meets the next incident link. Hence, up to an equivalence relation, the sectorization of a network, $\sigma \in \Gamma(\mathbf{K})$ is determined by whether a sectoring axis will be placed (instead of where exactly it will be placed) between adjacent undirected links of each node.

For node n , since a sectoring axis cannot be placed between the outgoing and incoming links corresponding to the same neighboring node of n , we consider undirected links regarding node n 's sectorization, σ_n . In the rest of the paper, let $\delta(n)$ denote the set of the undirected incident links of n , i.e., $\delta(n) = \{\ell_1, \dots, \ell_{|\delta(n)|}\}$, ordered in a way such that geometrically neighboring (consecutive) undirected links are next to each other. Note that $\ell_{|\delta(n)|}$ and ℓ_1 are also adjacent links due to the cyclic nature of σ_n . Using this notation, the sectorization of node n , $\sigma_n \in \Gamma_n(K_n)$, essentially partitions $\delta(n)$ into K_n non-overlapping subsets of links. We can also denote σ_n by placing the symbol “|” between two adjacent links where a sectoring axis is placed (e.g., $\delta_n = \{|(n, u), (n, v)\}$ in Fig. 5).

V. SECTORIZATION GAIN BASED ON NETWORK FLOW EXTENSION RATIO

In this section, we characterize the capacity region of sectorized networks and present the definitions of flow extension ratio and the corresponding sectorization gain. We consider a *general* sectorized network G^σ under sectorization $\sigma \in \Gamma(\mathbf{K})$ with given $\mathbf{K} \in \mathbb{Z}_+^N$, and its auxiliary graph H^σ . Let \mathcal{P}_{H^σ} be the matching polytope of H^σ .

We first present the following lemma that relates the convex hull of all feasible schedules in G^σ to \mathcal{P}_{H^σ} .

Lemma 1. *For a sectorized network G^σ and its auxiliary graph H^σ , let \mathcal{X}_{G^σ} be the set of feasible schedules in G^σ and \mathcal{M}_{H^σ} be the set of matchings in H^σ . Under the primary interference constraints, it holds that $\mathcal{X}_{G^\sigma} = \mathcal{M}_{H^\sigma}$ and $\text{Co}(\mathcal{X}_{G^\sigma}) = \text{Co}(\mathcal{M}_{H^\sigma}) = \mathcal{P}_{H^\sigma}$.*

Proof. First, we prove that $\mathcal{X}_{G^\sigma} \subseteq \mathcal{M}_{H^\sigma}$. For every feasible schedule \mathbf{X} in \mathcal{X}_{G^σ} , due to the way H^σ is constructed based on G^σ (see Section IV-A), $\exists \mathbf{M} \in \mathcal{M}_{H^\sigma}$ such that $\mathbf{X} = \mathbf{M}$. Next, we prove that $\mathcal{X}_{G^\sigma} \supseteq \mathcal{M}_{H^\sigma}$. Consider a matching $\mathbf{M} \in \mathcal{M}_{H^\sigma}$, it allows each node sector $\sigma_n^k, \forall n \in \mathcal{N}, \forall k \in [K_n]$ to be connected to at most one direct edge (see Section III-A). As a result, due to the primary interference constraints, \mathbf{M} is also a feasible schedule of G^σ . \square

Based on Lemma 1, the backpressure algorithm that obtains *maximum weight schedule (MWS)* $\mathbf{X}^{\text{BP}}(t)$ in G^σ (see Section III-D), which in general is NP-hard, is equivalent to finding the corresponding *maximum weight matching (MWM)* in H^σ , with the backpressure $\mathbf{D}(t)$ being the weights on the edges, i.e.,

$$\begin{aligned} \mathbf{X}^{\text{BP}}(t) &:= \arg \max_{\mathbf{X} \in \mathcal{X}_{G^\sigma}} \{\mathbf{D}^\top(t) \cdot \mathbf{X}\} \\ &= \arg \max_{\mathbf{M} \in \mathcal{M}_{H^\sigma}} \{\mathbf{D}^\top(t) \cdot \mathbf{M}\}. \end{aligned}$$

From Edmond's theory [29], [30], the MWM of H^σ can be obtained via a polynomial-time algorithm with complexity of $O(|V^\sigma|^2 \cdot |E|)$.

⁴A bipartite graph is a graph whose vertices can be divided into two *disjoint* and *independent* sets U_1 and U_2 such that every edge connects a vertex in U_1 to one in U_2 .

Intuitively, it is expected that G^σ under sectorization σ (with $H^\sigma = (V^\sigma, E^\sigma)$) has a capacity region that is at least the same as the unsectorized network G (with $H = (V, E)$), i.e., any network flow \mathbf{f} that can be maintained in the unsectorized network G can always be maintained in G^σ . This is proved by the following theorem.

Theorem 5.1. $\mathcal{P}_G = \mathcal{P}_H \subseteq \mathcal{P}_{H^\sigma}$, $\forall \mathbf{K} \in \mathbb{Z}_+^N$ and $\forall \sigma \in \Gamma(\mathbf{K})$.

Proof. Since $G \equiv H$, it holds that $\mathcal{P}_G = \mathcal{P}_H$. Consider a network flow $\mathbf{f} \in \mathcal{P}_G$, we will show that \mathbf{f} satisfies (7) for \mathcal{P}_{H^σ} . First, since $f_e \geq 0, \forall e \in E$, it holds that in H^σ , $f_e \geq 0, \forall e \in E^\sigma$. For $v \in V^\sigma$ corresponding to node $n \in \mathcal{N}$ with σ_n , note that $\sum_{e \in \delta(v)} f_e \leq \sum_{e \in \delta(n)} f_e \leq 1$. Second, we prove that $\sum_{e \in E(U')} f_e \leq \lfloor |U'|/2 \rfloor, \forall U' \subseteq V^\sigma$ with an odd cardinality $|U'|$. Let U' be an odd subset of vertices of V^σ and $U \subseteq \mathcal{N}$ denote the set of the corresponding nodes in \mathcal{N} from which the vertices in U' were deduced from. If $|U|$ is odd, the result easily follows since $\sum_{e \in E(U')} f_e \leq \sum_{e \in E(U)} f_e \leq \lfloor |U|/2 \rfloor \leq \lfloor |U'|/2 \rfloor$. If $|U|$ is even, let a node $n \in \mathcal{N}$ such that $n_k \in U'$ for a $k \in [K_n]$. Let $U'' = U \setminus \{n\}$ with an odd cardinality $|U''|$. Note that $\sum_{e \in E(U')} f_e \leq \sum_{e \in E(U'')} f_e + \sum_{e \in \delta(n)} f_e \leq \sum_{e \in E(U'')} f_e + 1 \leq \frac{|U''|-1}{2} + 1 \leq \frac{|U'| - 1}{2}$. The last inequality holds since $|U'| \geq |U''| + 1$ and both $|U'|$ and $|U''|$ are odd. \square

Based on (5) and Lemma 1, the capacity region of a sectorized network G^σ can be characterized by the matching polytope of its auxiliary graph, \mathcal{P}_{H^σ} . With a given (unknown) $\alpha \in \text{int}(\Lambda(G^\sigma))$ and a sectorization σ , the dynamic back-pressure algorithm will converge to and return a network flow vector $\mathbf{f} \in \mathcal{P}_{H^\sigma}$. We define the flow extension ratio, denoted by $\lambda^\sigma(\mathbf{f})$, which quantitatively measures *how much the network flow \mathbf{f} can be extended in its direction until it intersects the boundary of \mathcal{P}_{H^σ}* .

Definition 5.3 (Flow Extension Ratio). *For a sectorized network G^σ and network flow $\mathbf{f} \in \mathcal{P}_{H^\sigma}$, the flow extension ratio, $\lambda^\sigma(\mathbf{f})$, is the maximum scalar such that $\lambda^\sigma(\mathbf{f}) \cdot \mathbf{f} \in \mathcal{P}_{H^\sigma}$ still holds.*

Let $\zeta^\sigma(\mathbf{f}) := \min_{U \subseteq V^\sigma, |U| \text{ odd}} \left(\frac{\lfloor |U|/2 \rfloor}{\sum_{e \in E(U)} f_e} \right)$ (see (7)). With a little abuse of notation, for node n , network flow \mathbf{f} , and an undirected edge $e \in \delta(n)$ with directed components $e_+ \in \mathcal{L}_n^+$ and $e_- \in \mathcal{L}_n^-$, we let $f_e = f_{e_+} + f_{e_-}$. The flow extension ratio, $\lambda^\sigma(\mathbf{f})$, can be obtained by the following optimization problem:

$$\begin{aligned} \lambda^\sigma(\mathbf{f}) &:= \max_{\lambda \in \mathbb{R}^+} \lambda, \quad \text{s.t.: } \lambda \cdot \mathbf{f} \in \mathcal{P}_{H^\sigma} \\ &\stackrel{(7)}{=} \min \left\{ \min_{v \in V^\sigma} \frac{1}{\sum_{e \in \delta(v)} f_e}, \zeta^\sigma(\mathbf{f}) \right\}. \end{aligned} \quad (9)$$

Similarly, we define the flow extension ratio for the corresponding unsectorized network G , denoted by $\lambda^\varnothing(\mathbf{f}) := \max_{\lambda \in \mathbb{R}^+} \lambda$, s.t.: $\lambda \cdot \mathbf{f} \in \mathcal{P}_G$. Note that $\lambda^\varnothing(\mathbf{f})$ depends solely on the topology of G and is independent of the sectorization σ . Next, we define the *approximate flow extension ratio* with respect to the polytope \mathcal{Q}_{H^σ} .

Definition 5.4 (Approximate Flow Extension Ratio). *For a sectorized network G^σ and a network flow $\mathbf{f} \in \mathcal{P}_{H^\sigma}$, the*

approximate flow extension ratio, $\mu^\sigma(\mathbf{f})$, is the maximum scalar such that $\mu^\sigma(\mathbf{f}) \cdot \mathbf{f} \in \mathcal{Q}_{H^\sigma}$ still holds.

The following optimization problem determines $\mu^\sigma(\mathbf{f})$:

$$\begin{aligned} \mu^\sigma(\mathbf{f}) &:= \max_{\mu \in \mathbb{R}^+} \mu, \quad \text{s.t.: } \mu \cdot \mathbf{f} \in \mathcal{Q}_{H^\sigma} \\ &\stackrel{(8)}{=} \min_{v \in V^\sigma} \frac{1}{\sum_{e \in \delta(v)} f_e} = \frac{1}{\max_{v \in V^\sigma} \sum_{e \in \delta(v)} f_e}, \end{aligned} \quad (10)$$

We also define the approximate flow extension ratio for the unsectorized network G , denoted by $\mu^\varnothing(\mathbf{f}) := \max_{\lambda \in \mathbb{R}^+} \lambda$, s.t.: $\lambda \cdot \mathbf{f} \in \mathcal{Q}_G$.

To quantitatively evaluate the performance of a sectorization σ , we present the following definition of sectorization gains.

Definition 5.5 (Sectorization Gains). *The (explicit) sectorization gain of σ with a network flow \mathbf{f} is defined as $g_\lambda^\sigma(\mathbf{f}) := \frac{\lambda^\sigma(\mathbf{f})}{\lambda^\varnothing(\mathbf{f})}$ (with respect to \mathcal{P}_{H^σ}). The approximate sectorization gain of σ with a network flow \mathbf{f} is defined as $g_\mu^\sigma(\mathbf{f}) := \frac{\mu^\sigma(\mathbf{f})}{\mu^\varnothing(\mathbf{f})}$ (with respect to \mathcal{Q}_{H^σ}).*

The following lemma states the relationships between $\lambda^\sigma(\mathbf{f})$ and $\mu^\sigma(\mathbf{f})$, and between $g_\lambda^\sigma(\mathbf{f})$ and $g_\mu^\sigma(\mathbf{f})$. Parts (i) and (ii) of the Lemma can be found in [31] (Corollary of Section III).

Lemma 2. *For any sectorization σ and network flow \mathbf{f} , it holds that: (i) $\frac{2}{3} \cdot \mu^\sigma(\mathbf{f}) \leq \lambda^\sigma(\mathbf{f}) \leq \mu^\sigma(\mathbf{f})$, (ii) $\frac{1}{\mu^\sigma(\mathbf{f})} \geq \frac{1}{\lambda^\sigma(\mathbf{f})} - \max_{e \in E^\sigma} f_e$, and (iii) $\frac{2}{3} \cdot g_\mu^\sigma(\mathbf{f}) \leq g_\lambda^\sigma(\mathbf{f}) \leq \frac{3}{2} \cdot g_\mu^\sigma(\mathbf{f})$.*

Proof. (i) can be proved with the observation that in any (odd) subset $U \subseteq V^\sigma$, the cumulative weighted degree of any node cannot exceed $\frac{1}{\mu^\sigma(\mathbf{f})}$ by definition. It can also be proven from Shannon's result for chromatic indices [32], [31]. (ii) can be deduced from Vizing's theorem [33], [31], and (iii) is an immediate result of (i). \square

Remark 5.1. *If H^σ is a bipartite graph under sectorization σ , since the two polytopes \mathcal{Q}_{H^σ} and \mathcal{P}_{H^σ} are identical (see Section IV-C), it holds that $\lambda^\sigma(\mathbf{f}) = \mu^\sigma(\mathbf{f}), \forall \mathbf{f} \in \mathbb{R}^{|E|}$. See the discussions in Section VII for more details.*

VI. OPTIMIZATION AND A DISTRIBUTED APPROXIMATION ALGORITHM

Given a vector $\mathbf{K} \in \mathbb{Z}_+^N$, our objective is to find the sectorization $\sigma \in \Gamma(\mathbf{K})$ that maximizes the flow extension ratio, $\lambda^\sigma(\mathbf{f})$, under a network flow, \mathbf{f} . While the algorithm in this section focuses on a single, fixed sectorization, in Section VIII-B we present a dynamic routing approach that allows the network to re-sectorize in real time, adapting to the current network state. The aforementioned optimization problem, **(Opt)**, is given by:

$$\begin{aligned} \text{(Opt)} \quad \sigma^*(\mathbf{f}) &:= \arg \max_{\sigma \in \Gamma(\mathbf{K})} \lambda^\sigma(\mathbf{f}) \\ &\stackrel{(9)}{=} \arg \max_{\sigma \in \Gamma(\mathbf{K})} \left\{ \min \left\{ \min_{v \in V^\sigma} \frac{1}{\sum_{e \in \delta(v)} f_e}, \zeta^\sigma(\mathbf{f}) \right\} \right\}. \end{aligned} \quad (11)$$

We are optimizing towards the boundary of the matching polytope, \mathcal{P}_{H^σ} , over the set of sectorizations, $\Gamma(\mathbf{K})$, for a given network flow, \mathbf{f} . This is because there does not exist a single sectorization $\sigma \in \Gamma(\mathbf{K})$ that can achieve close-to-optimal performance of $\lambda^\sigma(\mathbf{f})$ for every network flow $\mathbf{f} \in \mathbb{R}^{|E|}$.

Algorithm 1 SECTORIZE- n for node n .

Input: K_n , $\delta(n)$, \mathbf{f}_n , and ϵ

- 1: $T_{\min} \leftarrow \max_{e \in \delta(n)} f_e$, $T_{\max} \leftarrow \sum_{e \in \delta(n)} f_e$, $T_{\text{temp}} \leftarrow 0$
- 2: $T_n^{\text{crit}} \leftarrow 0$, decision \leftarrow No
- 3: **while** $(T_{\max} - T_{\min}) > \epsilon$ **do**
- 4: $T_{\text{temp}} \leftarrow (T_{\min} + T_{\max})/2$
- 5: (decision, π_0) \leftarrow EXISTSECTORIZATION- $n(T_{\text{temp}})$ (Algorithm 2)
- 6: **if** decision = Yes **then**
- 7: $T_{\max} \leftarrow T_{\text{temp}}$
- 8: **else**
- 9: $T_{\min} \leftarrow T_{\text{temp}}$
- 10: **end if**
- 11: **end while**
- 12: $T_n^{\text{crit}} \leftarrow T_{\max}$
- 13: (decision, $\pi_n(\mathbf{f}_n)$) \leftarrow EXISTSECTORIZATION- $n(T_n^{\text{crit}})$
- 14: **return** The sectorization for node n , $\pi_n(\mathbf{f}_n)$

Algorithm 2 EXISTSECTORIZATION- $n(T)$ for node n .

Input: K_n , $\delta(n)$, \mathbf{f}_n , and T

- 1: **for** $e \in \delta(n)$ **do**
- 2: Reset node n 's sectorization $\pi_n \leftarrow \emptyset$
- 3: Put a sectorizing axis in π_n right after e (clockwise)
- 4: sectors_needed $\leftarrow 1$, total_weight $\leftarrow 0$
- 5: $e' \leftarrow$ the edge next to e in $\delta(n)$ (clockwise)
- 6: **while** $e' \neq e$ **do**
- 7: **if** $f_{e'} > T$ **then return** (No, \emptyset)
- 8: **else**
- 9: total_weight \leftarrow total_weight + $f_{e'}$
- 10: **if** total_weight $> T$ **then**
- 11: sectors_needed \leftarrow sectors_needed + 1
- 12: Put a sectorizing axis in π_n before e' (counter-clockwise)
- 13: total_weight $\leftarrow f_{e'}$
- 14: **end if**
- 15: $e' \leftarrow$ the edge next to e in $\delta(n)$ (clockwise)
- 16: **end if**
- 17: **end while**
- 18: **if** sectors_needed $\leq K_n$ **then**
- 19: **return** (Yes, π_n)
- 20: **end if**
- 21: **end for**
- 22: **return** (No, \emptyset)

A. Key Insight and Intuition

In general, (**Opt**) is analytically intractable due to its combinatorial nature and the fact that $\zeta^\sigma(\mathbf{f})$ needs exponentially many calculations even for a fixed sectorization σ . Instead, we consider an alternative optimization problem:

$$(\mathbf{Opt-Approx}) \quad \tilde{\sigma}(\mathbf{f}) := \arg \max_{\sigma \in \Gamma(\mathbf{K})} \mu^\sigma(\mathbf{f})$$

$$\stackrel{(10)}{=} \arg \max_{\sigma \in \Gamma(\mathbf{K})} \left\{ \min_{v \in V^\sigma} \frac{1}{\sum_{e \in \delta(v)} f_e} \right\}. \quad (12)$$

Although (**Opt-Approx**) excludes the constraint $\zeta^\sigma(\mathbf{f})$ in (**Opt**), solving it by a brute-force algorithm is still analytically intractable due to the coupling between the (possibly different) sectorization of *all* nodes. For example, if each of the N nodes has \tilde{K} possible sectorizations, a total number of $N^{\tilde{K}}$ sectorizations need to be evaluated to solve (**Opt-Approx**).

Our key insight behind developing a distributed approximation algorithm (described in Section VI-B) is that (**Opt-**

Approx) can be decomposed into N individual optimization problems, (**Opt-Approx- n**), for each node $n \in \mathcal{N}$. With a little abuse of notation, let $\mathbf{f}_n = (f_e : e \in \delta(n))$ be the ‘‘local’’ flows on the undirected edges incident to node n . This decomposed optimization problem is given by:

$$(\mathbf{Opt-Approx-}n) \quad \mathbf{v}_n(\mathbf{f}_n)$$

$$:= \arg \min_{\sigma_n \in \Gamma_n(K_n)} \max_{v \in \{n_1^{\sigma_n}, \dots, n_{K_n}^{\sigma_n}\}} \sum_{e \in \delta(v)} f_e. \quad (13)$$

(**Opt-Approx- n**) determines node n 's sectorization, $\mathbf{v}_n(\mathbf{f}_n)$, based on its local flows, \mathbf{f}_n , and is *independent* of the other nodes. The following lemma shows that the sectorization obtained by solving the N decomposed problems, (**Opt-Approx- n**), is equivalent to that obtained by solving (**Opt-Approx**).

Lemma 3. For a given network flow \mathbf{f} , the sectorization $\mathbf{v}(\mathbf{f})$, which consists of the solutions of (**Opt-Approx- n**) for all nodes $n \in \mathcal{N}$, is equivalent to the solution $\tilde{\sigma}(\mathbf{f})$ to (**Opt-Approx**), i.e.,

$$\tilde{\sigma}(\mathbf{f}) = \mathbf{v}(\mathbf{f}) = (\mathbf{v}_1(\mathbf{f}_1), \dots, \mathbf{v}_N(\mathbf{f}_N)) \text{ and } \mu^\mathbf{v}(\mathbf{f}) = \mu^{\tilde{\sigma}}(\mathbf{f}). \quad (14)$$

Proof. The key observation is that the sectorization of node n , σ_n , affects only the values of $\{\sum_{e \in \delta(n_1^{\sigma_n})} f_e, \dots, \sum_{e \in \delta(n_{K_n}^{\sigma_n})} f_e\}$, for nodes $\{n_1^{\sigma_n}, \dots, n_{K_n}^{\sigma_n}\} \subseteq V^\sigma$ in the auxiliary graph H^σ , respectively. Therefore, it holds that

$$\begin{aligned} \tilde{\sigma}(\mathbf{f}) &\stackrel{(12)}{=} \arg \max_{\sigma \in \Gamma(\mathbf{K})} \mu^\sigma(\mathbf{f}) \\ &\stackrel{(10)}{=} \arg \max_{\sigma \in \Gamma(\mathbf{K})} \left\{ \min_{v \in V^\sigma} \frac{1}{\sum_{e \in \delta(v)} f_e} \right\} \\ &= \arg \min_{(\sigma_1, \dots, \sigma_N) \in \Gamma(\mathbf{K})} \left\{ \max_{v \in V^\sigma} \sum_{e \in \delta(v)} f_e \right\} \\ &= \arg \min_{(\sigma_1, \dots, \sigma_N) \in \Gamma(\mathbf{K})} \left\{ \max_{n \in \mathcal{N}} \left\{ \max_{k \in [K_n]} \sum_{e \in \delta(n_k^{\sigma_n})} f_e \right\} \right\} \\ &= \left[\arg \min_{\sigma_n \in \Gamma_n(K_n)} \left\{ \max_{v \in \{n_1^{\sigma_n}, \dots, n_{K_n}^{\sigma_n}\}} \sum_{e \in \delta(v)} f_e \right\} : \forall n \in \mathcal{N} \right] \\ &\stackrel{(13)}{=} (\mathbf{v}_1(\mathbf{f}_1), \dots, \mathbf{v}_N(\mathbf{f}_N)) = \mathbf{v}(\mathbf{f}). \end{aligned} \quad (15)$$

Since $\tilde{\sigma}(\mathbf{f}) = \mathbf{v}(\mathbf{f})$, it also holds that $\mu^\mathbf{v}(\mathbf{f}) = \mu^{\tilde{\sigma}}(\mathbf{f})$ (see (10)). Note that the second-to-last equation in (15) holds because the corresponding problem is separable. \square

Although (**Opt-Approx- n**) is a distributed optimization problem for each node n , to solve it using a brute-force method still remains high complexity. Consider the sectorization of node n with $|\delta(n)|$ incident edges into K_n sectors ($|\delta(n)| \leq (N-1)$). To solve (**Opt-Approx- n**) in a brute-force way, a total number of $\binom{|\delta(n)|}{K_n} = O\left(\binom{N}{K_n}\right) = O(N^{K_n})$ possible sectorizations need to be enumerated. Next, we present a polynomial-time distributed algorithm that solves (**Opt-Approx- n**) with a complexity independent of K_n .

B. A Distributed Approximation Algorithm

We now present a distributed approximation algorithm, SECTORIZE- n , that efficiently solves (**Opt**) with guaranteed performance. In essence, SECTORIZE- n solves (**Opt-Approx- n**) for each individual node $n \in \mathcal{N}$. Algorithm 1 presents

the pseudocode for SECTORIZE- n , which includes two main components:

(1) A **decision problem**, EXISTSECTORIZATION- $n(T)$, that determines the *existence* of a sectorization for node n (with K_n , $\delta(n)$, and \mathbf{f}_n) under a given threshold value, $T \in \mathbb{R}_+$, given by

$$\text{EXISTSECTORIZATION-}n(T) = \begin{cases} (\mathbf{Yes}, \mathbf{v}_0), & \text{if } \exists \mathbf{v}_0 \in \Gamma_n(K_n) : \max_{v \in \{n_1^{\mathbf{v}_0}, \dots, n_{K_n}^{\mathbf{v}_0}\}} \sum_{e \in \delta(v)} f_e \leq T, \\ (\mathbf{No}, \emptyset), & \text{if } \forall \mathbf{v}_0 \in \Gamma_n(K_n) : \max_{v \in \{n_1^{\mathbf{v}_0}, \dots, n_{K_n}^{\mathbf{v}_0}\}} \sum_{e \in \delta(v)} f_e > T. \end{cases} \quad (16)$$

EXISTSECTORIZATION- $n(T)$ can be solved as follows. Consider the set of edges incident to node n , $\delta(n) = (e'_1, \dots, e'_{|\delta(n)|})$. We begin by assuming that the first sectoring axis of node n is placed between its first and last incident edge, i.e., $(|e'_1, \dots, e'_{|\delta(n)|}|)$. Under this assumption, the second sectoring axis will be placed between the k^{th} and $(k+1)^{\text{th}}$ incident edges if $\sum_{i=1}^k f_{e'_i} \leq T$ and $\sum_{i=1}^{k+1} f_{e'_i} > T$. Then, the process is repeated for the remaining edges $\delta(n) \setminus \{e_1, \dots, e_k\}$ to find the third sectoring axis, so on and so forth until all edges in $\delta(n)$ are enumerated for the threshold, T . Although the above procedure started by placing the first sectoring axis arbitrarily, correctness is ensured by repeating this process for all $|\delta(n)|$ possible initial positions between incident edges.

(2) A **binary search process** that finds the critical threshold, T_n^{crit} , based on which the optimized sectorization for node n , denoted by π_n , is determined by EXISTSECTORIZATION- $n(T_n^{\text{crit}})$.

The following theorem states our main results regarding the correctness of SECTORIZE- n and its guaranteed performances as a distributed approximation algorithm.

Theorem 6.2. *For a given network flow \mathbf{f} , it holds that:*

(i) [**Correctness**] *The sectorization of node n returned by SECTORIZE- n , $\pi_n(\mathbf{f}_n)$, is equivalent to $\mathbf{v}_n(\mathbf{f}_n)$ in (Opt-Approx- n), i.e.,*

$$\pi_n(\mathbf{f}_n) = \mathbf{v}_n(\mathbf{f}_n), \quad \forall n \in \mathcal{N}, \quad (17)$$

(ii) [**Approximation Ratio**] *The distributed SECTORIZE- n algorithm is a 2/3-approximation algorithm, i.e.,*

$$\frac{2}{3} \leq \frac{\lambda^{\pi}(\mathbf{f})}{\lambda^{\sigma^*}(\mathbf{f})} \leq 1, \quad (18)$$

where $\lambda^{\sigma^*}(\mathbf{f})$ is flow extension ratio achieved by the optimal sectorization as the solution to (Opt).

Proof. First, we prove (i). We show that the decision returned by EXISTSECTORIZATION- $n(T)$ has a monotonic property with respect to T , i.e., there exists a critical threshold, $T_n^{\text{crit}} \in \mathbb{R}_+$, such that

$$\text{EXISTSECTORIZATION-}n(T) = \begin{cases} (\mathbf{No}, \emptyset), & \forall T \in [0, T_n^{\text{crit}}), \\ (\mathbf{Yes}, \cdot), & \forall T \in [T_n^{\text{crit}}, +\infty). \end{cases} \quad (19)$$

It is easy to see that EXISTSECTORIZATION- $n(T)$ outputs \mathbf{No} for $T = 0$ and \mathbf{Yes} for a sufficiently large T with a non-zero flow \mathbf{f} . Let T_n^{crit} be the smallest T such that $\exists \pi_n \in \Gamma_n(K_n)$

with which the output of (16) is (\mathbf{Yes}, π_n) . As a result, we have $\text{EXISTSECTORIZATION-}n(T) = (\mathbf{No}, \emptyset)$, $\forall T \in [0, T_n^{\text{crit}})$. In addition, π_n and T_n^{crit} satisfy

$$\max_{v \in \{n_1^{\pi_n}, \dots, n_{K_n}^{\pi_n}\}} \sum_{e \in \delta(v)} f_e \leq T, \quad \forall T \in [T_n^{\text{crit}}, +\infty).$$

Therefore, for a network flow \mathbf{f}_n incident to node n , we can set

$$T_n^{\text{crit}} = \min_{\sigma_n \in \Gamma_n(K_n)} \left\{ \max_{v \in \{n_1^{\sigma_n}, \dots, n_{K_n}^{\sigma_n}\}} \sum_{e \in \delta(v)} f_e \right\}, \quad (20)$$

and the sectorization of node n corresponding to T_n^{crit} is equivalent to \mathbf{v}_n in (Opt-Approx- n), i.e.,

$$\pi_n(\mathbf{f}) = \arg \min_{\sigma_n \in \Gamma_n(K_n)} \left\{ \max_{v \in \{n_1^{\sigma_n}, \dots, n_{K_n}^{\sigma_n}\}} \sum_{e \in \delta(v)} f_e \right\} \stackrel{(13)}{=} \mathbf{v}_n(\mathbf{f}_n). \quad (21)$$

Due to the monotonicity of (19), the critical value T_n^{crit} can be found via a binary search within the interval $[\max_{e \in \delta(n)} f_e, \sum_{e \in \delta(n)} f_e]$ with a sufficiently small ϵ , which is a parameter that controls the trade-offs between accuracy and convergence of Algorithm 1. Then, $\pi_n(\mathbf{f}_n)$ can be obtained via EXISTSECTORIZATION- $n(T_n^{\text{crit}})$.

Next, we prove (ii). For a network flow \mathbf{f} , consider the sectorizations $\sigma^*(\mathbf{f})$ and $\tilde{\sigma}(\mathbf{f})$ as the solution to (Opt) and (Opt-Approx), respectively. It is easy to see from their definitions that $\lambda^{\pi}(\mathbf{f}) \leq \lambda^{\sigma^*}(\mathbf{f}) \Rightarrow \frac{\lambda^{\pi}(\mathbf{f})}{\lambda^{\sigma^*}(\mathbf{f})} \leq 1$. From (11)–(12) and Lemma 2, we have

$$\lambda^{\sigma^*}(\mathbf{f}) \leq \mu^{\sigma^*}(\mathbf{f}) \leq \mu^{\tilde{\sigma}}(\mathbf{f}) \text{ and } \frac{2}{3} \cdot \mu^{\tilde{\sigma}}(\mathbf{f}) \leq \lambda^{\tilde{\sigma}}(\mathbf{f}), \quad (22)$$

which further implies that

$$\frac{2}{3} \cdot \lambda^{\sigma^*}(\mathbf{f}) \leq \frac{2}{3} \cdot \mu^{\tilde{\sigma}}(\mathbf{f}) \leq \lambda^{\tilde{\sigma}}(\mathbf{f}). \quad (23)$$

In addition, since $\pi(\mathbf{f}) = \mathbf{v}(\mathbf{f}) = \tilde{\sigma}(\mathbf{f})$ (see Theorem 6.2 (i) and Lemma 3), we can conclude that

$$\frac{2}{3} \cdot \lambda^{\sigma^*}(\mathbf{f}) \leq \lambda^{\tilde{\sigma}}(\mathbf{f}) = \lambda^{\pi}(\mathbf{f}) \Rightarrow \frac{\lambda^{\pi}(\mathbf{f})}{\lambda^{\sigma^*}(\mathbf{f})} \geq \frac{2}{3}, \quad (24)$$

and Theorem 6.2 (ii) follows directly. \square

Remark 6.2 (Complexity of SECTORIZE- n). Recall from the proof of Theorem 6.2 that $T_n^{\text{crit}} \in [\max_{e \in \delta(n)} f_e, \sum_{e \in \delta(n)} f_e]$. Let $\Theta := (\sum_{e \in \delta(n)} f_e - \max_{e \in \delta(n)} f_e) / \epsilon$, the binary search process of SECTORIZE- n will terminate in $O(\log_2 \Theta)$ iterations, and each iteration has a complexity of $O(|\delta(n)|^2)$ (see Algorithm 2). Therefore, the complexity of SECTORIZE- n is $O(|\delta(n)|^2 \cdot \log_2 \Theta) = O(N^2 \cdot \log_2 \Theta)$.

Remark 6.3. Based on Lemma 2, we can obtain another lower bound of the approximation ratio of SECTORIZE- n given by:

$$\frac{\lambda^{\pi}(\mathbf{f})}{\lambda^{\sigma^*}(\mathbf{f})} \geq \frac{1}{1 + \lambda^{\sigma^*}(\mathbf{f}) \cdot \max_{e \in E} f_e} \geq \frac{1}{1 + \mu^{\pi}(\mathbf{f}) \cdot \max_{e \in E} f_e} := LB^{\pi}(\mathbf{f}). \quad (25)$$

Proof. Lemma 2(ii) for $\sigma = \pi$ gives,

$$\frac{1}{\mu^{\pi}(\mathbf{f})} \geq \frac{1}{\lambda^{\pi}(\mathbf{f})} - \max_{e \in E} f_e. \quad (26)$$

By definition of sectorization π and Lemma 2(i), we have $\mu^{\pi}(\mathbf{f}) \geq \mu^{\sigma^*}(\mathbf{f}) \geq \lambda^{\sigma^*}(\mathbf{f})$ and hence $\frac{1}{\lambda^{\sigma^*}(\mathbf{f})} \geq \frac{1}{\mu^{\pi}(\mathbf{f})}$.

Therefore, (26) becomes

$$\frac{1}{\lambda^\pi(\mathbf{f})} - \max_{e \in E} f_e \leq \frac{1}{\lambda^{\sigma^*}(\mathbf{f})} \Leftrightarrow \frac{\lambda^{\sigma^*}(\mathbf{f})}{\lambda^\pi(\mathbf{f})} \leq 1 + \lambda^{\sigma^*}(\mathbf{f}) \cdot \max_{e \in E} f_e$$

which gives the final result:

$$\frac{\lambda^\pi(\mathbf{f})}{\lambda^{\sigma^*}(\mathbf{f})} \geq \frac{1}{1 + \lambda^{\sigma^*}(\mathbf{f}) \cdot \max_{e \in E} f_e}.$$

The second inequality of (25) follows using the inequality $\mu^\pi(\mathbf{f}) \geq \mu^{\sigma^*}(\mathbf{f}) \geq \lambda^{\sigma^*}(\mathbf{f})$. \square

This bound is useful since, from the definition of $\lambda^{\sigma^*}(\mathbf{f})$, i.e., the extension ratio of \mathbf{f} for it “hit” the boundary of $\mathcal{P}_{H^{\sigma^*}}$, the values of $\lambda^{\sigma^*}(\mathbf{f})$ and $\max_{e \in E^{\sigma^*}} f_e$ can not be large simultaneously. Although $\lambda^{\sigma^*}(\mathbf{f})$ is analytically intractable, since $\lambda^{\sigma^*}(\mathbf{f}) \leq \mu^{\sigma^*}(\mathbf{f}) \leq \mu^\pi(\mathbf{f})$, we can derive another lower bound of the approximation ratio, $LB^\pi(\mathbf{f})$, which depends on $\mu^\pi(\mathbf{f})$. Note that $LB^\pi(\mathbf{f})$ is tractable since $\max_{e \in E^{\sigma^*}} f_e$ is independent of the sectorization and $\mu^\pi(\mathbf{f})$ can be explicitly computed (10). In other words,

$$\max \left\{ \frac{2}{3}, LB^\pi(\mathbf{f}) \right\} \leq \frac{\lambda^\pi(\mathbf{f})}{\lambda^{\sigma^*}(\mathbf{f})} \leq 1. \quad (27)$$

In Section IX-B, we show that for small values of K_n , $LB^\pi(\mathbf{f})$ is indeed a much tighter bound than $2/3$ in (18).

Discussions and Applications. The distributed SECTORIZE- n algorithm approximates the optimal sectorization, $\sigma^*(\mathbf{f})$, which maximizes the flow extension ratio, $\lambda^\sigma(\mathbf{f})$, under given \mathbf{f} and $\mathbf{K} \in \mathbb{Z}_+^N$. The choice of a sectorization should be based on a network flow, \mathbf{f} as the polytope \mathcal{P}_{H^σ} can be augmented in different flow directions depending on σ . Hence, different sectorizations favor different sets of network flows. Some discussions about the proposed optimization framework:

- *Known Arrival Rates.* In the case with single-hop traffic, the capacity region of a network G^σ is given by $\Lambda(G^\sigma) = \text{Co}(\mathcal{X}_{G^\sigma})$ (see (5)). With a known arrival rate matrix α , SECTORIZE- n augments the capacity region with respect to the required α . Similarly, in the case of multi-hop traffic, with a known α , one can first obtain a feasible multi-commodity network flow \mathbf{f} that supports α , and then augment the polytope \mathcal{P}_{H^σ} according to this \mathbf{f} .
- *Varying the Number of Sectors.* With proper (minor) modifications, SECTORIZE- n can also return the minimum number of sectors K_n for every node n such that a given network flow, \mathbf{f} , can be maintained by the network, i.e., $\mathbf{f} \in \mathcal{P}_{H^\sigma}$. This is due to the distributed nature the proposed optimization framework, (**Opt-Approx- n**). Compared to previous work (e.g., [31]) whose objective is to obtain the minimum rate required for a network to support a flow vector \mathbf{f} , our proposed framework also provides a method to support \mathbf{f} via efficient sectorization based on available resources.
- *Changing the Effective Topology of the Network.* A natural question that arises after developing the proposed optimization framework is whether the network can be sectorized in a way to embed a specific useful structural property in its auxiliary graph, such that the underlying links between nodes can be changed. Since in the sectorized network, the routing and scheduling schemes can be run conceptually in

the auxiliary graph rather than in the connectivity graph, by choosing specific sectorizations the network architect might be able to induce properties in the graph to boost the performance of the algorithms to be executed in the network. For example, some sectorization schemes could potentially divide the network into conceptual non-communicating clusters or make the auxiliary graph bipartite.

VII. BIPARTITE AUXILIARY GRAPHS & EVEN HOMOGENEOUS SECTORIZATION

As a special case of changing the effective topology using sectorization, in this section, we present the class of *Even Homogeneous Sectorizations*, under which the auxiliary graph of a network, H^σ , is guaranteed to be bipartite.

A. Motivation for Inducing Bipartiteness in H^σ

For a network G and $\mathbf{K} \in \mathbb{Z}_+^N$, let $\Gamma_{bi}(\mathbf{K})$ be the set of network sectorizations such that the auxiliary graph H^σ is a bipartite graph, $\forall \sigma \in \Gamma_{bi}(\mathbf{K})$. We are particularly interested in the network sectorizations $\Gamma_{bi}(\mathbf{K})$ because of two main reasons. First, recall from section IV-C that the matching polytope and fractional matching polytope of a bipartite graph G_{bi} are equivalent, i.e., $\mathcal{P}_{G_{bi}} = \mathcal{Q}_{G_{bi}}$. A sectorized network with a bipartite auxiliary graph, H^σ , (and an unsectorized network with a bipartite connectivity graph) have a significantly simplified explicit capacity region characterization given by its fractional matching polytope \mathcal{Q}_{H^σ} , since $\mathcal{P}_{H^\sigma} = \mathcal{Q}_{H^\sigma}$ (see (8) and Lemma 1). Second, the maximum weight matching (MWM) in H^σ used as part of the backpressure algorithm, described in section V, can be obtained more efficiently when H^σ is a bipartite graph (see [29] for a detailed survey). Moreover, the MWM in a bipartite graph can be obtained in a distributed manner [34], which is suitable for wireless networks where nodes have only local information. In that way, the routing can be achieved in a distributed manner.

One intuitive way to construct a network sectorization $\sigma \in \Gamma_{bi}(\mathbf{K})$ is to set $K_n = |\delta(n)|, \forall n$ and put each link in $\delta(n)$ in a separate sector, i.e., $\sigma_n = \{|\ell_1| \ell_2| \dots | \ell_{|\delta(n)|}\}, \forall n$. However, we might not be able to afford that many sectors for every node. Next, we present a class of network sectorizations under which the auxiliary graph of the sectorized network is *guaranteed* to be bipartite for any even $K_1 = \dots = K_N$, therefore enjoying the benefits described above.

B. Even Homogeneous Sectorization

We now present the class of *Even Homogeneous Sectorizations*, denoted by $\mathcal{H}(K) \subseteq \Gamma(\mathbf{K})$ for $K \in \mathbb{Z}_+$ and $\mathbf{K} = (K, \dots, K) \in \mathbb{Z}_+^N$. For a network G^σ with sectorization $\sigma \in \mathcal{H}(K)$: (i) every node has the same even number of sectors, i.e., $K_n = K, \forall n$ with an even number K , (ii) all the K sectors of a node have an equal FoV of $360^\circ/K$, and (iii) at least one sectoring axis (and hence all sectoring axes) are parallel across the nodes. Although (ii) and (iii) may seem restrictive, based on the notion of equivalent sectorization described in section IV-D, our results that hold for all sectorizations in $\mathcal{H}(K)$ also hold for their corresponding equivalent sectorizations in $\Gamma(\mathbf{K})$.

The following lemma shows that for a sectorized network G^σ with $\sigma \in \mathcal{H}(K)$, its auxiliary graph H^σ is bipartite.

Lemma 4. *For a sectorized network G^σ with an Even Homogeneous Sectorization $\sigma \in \mathcal{H}(K)$ and $K \in \mathbb{Z}_+$, its auxiliary graph H^σ is bipartite. Moreover, H^σ consists of $K/2$ isolated bipartite graphs.*

Proof. Without loss of generality, we assume that the parallel sectoring axes across different nodes are labeled with the same index, i.e., for a given $k \in [K]$, $\{\eta_n^k : \forall n\}$ is a set of parallel sectoring axes. Recall from section III-A that for node n , we call the boundary of two adjacent sectors k and $(k+1)$ a *sectoring axis* and denote it by η_n^k . We define the sectoring axis between sector K and sector 1 with η_n^K . We also assume that for node n , its sectoring axes are indexed from $k=1$ to K clockwise. Using simple geometric calculations, it can be shown that under even homogeneous sectorization $\sigma \in \mathcal{H}(K)$, the k^{th} sector of node n , σ_n^k , can only share a link in \mathcal{L}^σ , with the k^{th} sector of node n' , $\sigma_{n'}^{k'}$, $\forall n' \in V, n' \neq n, \forall k \in [K]$, where k' necessarily satisfies

$$k' = (k + K/2) \bmod K.$$

As a result, in the auxiliary graph $H^\sigma = (V^\sigma, E^\sigma)$ (see section IV-A), the vertices in V^σ associated with the k^{th} sector of node n can only be connected with the vertices in V^σ associated with the k^{th} sector of node $n' \in \mathcal{N}, n' \neq n$, and vice versa. Therefore, H^σ is a bipartite graph and consists of $K/2$ completely isolated bipartite graphs. \square

Note that Lemma 4 has the following implications on the complexity of obtaining the MWM in the backpressure algorithm and hence the stabilization of the network. Let $NB(|V|, |E|, W)$ denote time complexity of obtaining the MWM in a general (non-bipartite) graph $G = (V, E)$, and $B(|V_{bi}|, |E_{bi}|, W)$ denote the time complexity of obtaining the MWM in a bipartite graph $G_{bi} = (V_{bi}, E_{bi})$, where $W := \|\mathbf{w}\|_\infty$ is the maximum value in the integer-valued edge weight vector \mathbf{w} of the corresponding graph. In our case, the weight on each edge is its backpressure (see section III-D). It is known that with the same values of $|V|$, $|E|$, and W , $B(|V|, |E|, W)$ is asymptotically better than $NB(|V|, |E|, W)$ (e.g., see [29]). We present the following theorem.

Theorem 7.3. *For an unsectorized network $G = (\mathcal{N}, \mathcal{L})$ with $|\mathcal{N}| = N$ and $|\mathcal{L}| = L$, each iteration of the dynamic backpressure algorithm needs an algorithm of time complexity $NB(N, L, W)$ to obtain the MWM in G . When the network is sectorized with an Even Homogeneous Sectorization $\sigma \in \mathcal{H}(K)$ to construct G^σ (with its auxiliary graph H^σ), each iteration of the dynamic backpressure algorithm needs $K/2$ distributed computations of an algorithm of $B(N, L, W)$ time complexity to obtain the MWM in H^σ .*

Proof. For a sectorized network G^σ with even homogeneous sectorization $\sigma \in \mathcal{H}(K)$, in order to compute the asymptotic complexity of each iteration of the dynamic backpressure algorithm, we should think about each bipartite subgraph in the auxiliary graph, H^σ , separately. Lemma 4 shows that H^σ can be divided into $K/2$ isolated subgraphs, all of which are bipar-

title. In every bipartite subgraph, each partition set consists of all the auxiliary nodes associated with the same sector in the sectorized network G^σ . In particular, each bipartite subgraph is composed of two sets of vertices: the first set consists of the auxiliary nodes that correspond to a sector $k \in [K]$, and the second set consist of the auxiliary nodes that correspond to the sector $(k + K/2) \bmod K$. Therefore, each bipartite subgraph consists of $\frac{2|V^\sigma|}{K} = \frac{2K|\mathcal{N}|}{K} = 2N$ vertices. For the edges, we can deduce that the $|\mathcal{L}| = L$ number of edges of G^σ are divided and distributed across the $K/2$ bipartite subgraphs. The specific distribution of the edges between the subgraphs depends on the network sectorization and the topology of G^σ .

For the dynamic backpressure algorithm in G^σ in each time slot, we should simply calculate the MWM of these $K/2$ isolated bipartite subgraphs. Let us distinguish these isolated bipartite subgraphs by subscript $b \in [K/2]$. Let V_b^σ , E_b^σ , and W_b denote the set of nodes, set of edges, and the maximum edge weight in the b^{th} isolated bipartite subgraph of H^σ , respectively. Then, obtaining the MWM in the b^{th} bipartite subgraph required an algorithm with time complexity $B(|V_b^\sigma|, |E_b^\sigma|, W_b)$ where $|E_b^\sigma| \leq L$ and $W_b \leq W$. Note that since the $K/2$ bipartite subgraphs are completely isolated, we can calculate the MWM in each of them in parallel. \square

Lemma 4 and Theorem 7.3 show that the MWM can be obtained by a distributed algorithm among $K/2$ isolated bipartite subgraphs and, in addition, in every bipartite subgraph, the MWM can be obtained distributedly across the nodes in that subgraph (e.g., according to [34]). More importantly, it is implied that sectorizing the network with $\sigma \in \mathcal{H}(K)$ can *simultaneously* improve the network capacity and reduce the complexity required for every iteration of the backpressure algorithm. Since the backpressure algorithm is dynamic and is executed in each time slot, we can achieve significant improvement in the overall efficiency when stabilizing the considered sectorized network.

Having shown that the set of even homogeneous sectorizations, \mathcal{H} , is beneficial regarding the complexity and time required for stabilizing the network, we now take a second look at **(Opt)** and **(Opt-Approx)**. From section IV-C and Remark 5.1, when the network sectorization is optimized over $\mathcal{H}(K) \subseteq \Gamma(\mathbf{K})$, since $\mathcal{P}_{H^\sigma} = \mathcal{Q}_{H^\sigma}$, it holds that for a given network flow \mathbf{f} and $\forall K \in \mathbb{Z}_+$,

$$\lambda^\sigma(\mathbf{f}) = \mu^\sigma(\mathbf{f}), \forall \sigma \in \mathcal{H}(K),$$

and therefore, the network sectorization optimized over the set $\mathcal{H}(K)$, denoted by $\hat{\sigma}(\mathbf{f})$, is given by

$$\hat{\sigma}(\mathbf{f}) := \arg \max_{\sigma \in \mathcal{H}(K)} \lambda^\sigma(\mathbf{f}) = \arg \max_{\sigma \in \mathcal{H}(K)} \mu^\sigma(\mathbf{f}).$$

This reveals the trade-offs between the optimality of the obtained sectorization (i.e., $\hat{\sigma}$ compared with σ^*) and the time complexity required for obtaining the MWM in the dynamic backpressure algorithm (i.e., optimization over the set of $\mathcal{H}(K)$ compared with over the set of $\Gamma(\mathbf{K})$).

VIII. JOINT ROUTING, SCHEDULING, AND DYNAMIC SECTORIZATION

In Section V, we presented the throughput-optimal policy for a single sectorization scenario, and in Section VI, we optimize the choice of sectorization to maximize the capacity in a single direction. Additionally, in Section VII, we introduced the case of Even Homogeneous Sectorization, where all nodes are sectorized uniformly, ensuring that the auxiliary graph is bipartite. This bipartite structure not only simplifies scheduling but also accelerates network stabilization compared to unsectorized networks. These approaches demonstrate the power of sectorization, but they assume a fixed configuration that is not to be changed throughout the network operation.

Furthermore, recent advancements in electronically and/or mechanically steerable antenna arrays might enable the capability to change sectorization over time in a practical manner. This capability enables the network to dynamically leverage capacity increases in multiple flow directions simultaneously,⁵ leading to an overall enhancement in end-to-end capacity by combining multiple optimal sectorization states instead of committing to a single configuration. This raises a fundamental question: What happens if the sectorizations can be changed dynamically? In such cases, a dynamic sectorization strategy that adapts to the network state is necessary to fully exploit the benefits of sectorized wireless networks. Below, we present an opportunistic dynamic sectorization approach that leverages our proposed sectorization algorithm (Section VIII-A), and provide a throughput optimal policy for joint sectorization, scheduling, and routing (Section VIII-B).

A. Opportunistic Dynamic Sectorization via Backpressure-Driven Optimization

This approach first leverages the backpressure algorithm to establish a current network flow. Once this flow is determined,⁶ we apply our optimization framework to select the most effective sectorization configuration given the prevailing traffic conditions. Instead of performing sectorization jointly with routing and scheduling in each time slot, this method allows the backpressure algorithm to first indicate a network flow and depending on how frequently we can adjust the sectorization, we can optimize it.

More specifically, starting with an (unknown and/or time-varying) arrival rate matrix $\alpha \in \text{int}(\Lambda(G^\sigma))$ and a given sectorization $\sigma \in \Gamma(\mathbf{K})$, the dynamic backpressure algorithm will converge to and return a network flow $\mathbf{f} \in \mathcal{P}_{H^\sigma}$. Using the proposed framework, one can find the sectorization that approximates the best sectorization with respect to \mathbf{f} . The rationale behind this is that the sectorized network will be able to maintain arrival rates proportionally higher than α . Moreover, when $\lambda^{\bar{\sigma}}(\mathbf{f})$ is analytically tractable, it can provide information about how much \mathbf{f} can be extended until it intersects with the boundary of the matching polytope

⁵Allowing dynamic sectorization enables the network to achieve a capacity region that is the convex hull of the capacities associated with fixed sectorization configurations, effectively expanding the achievable throughput.

⁶The network flow can be estimated by averaging observed link flows over time.

\mathcal{P}_{H^σ} . Therefore, the proposed framework can enable *dynamic sectorization* of the network to adapt to every network flow \mathbf{f} obtained by the backpressure algorithm, including in scenarios with time-varying arrival rates, α .

While this method is not throughput-optimal, it provides a structured approach to optimizing sectorization periodically based on the current network state and as shown in Section IX is faster than the throughput optimal algorithm proposed in the next section.

B. Optimal Joint Sectorization, Routing, and Scheduling

In Section V, we formulated backpressure routing as the joint throughput-optimal scheduling and routing with fixed sectorization. However, with dynamic sectorization, the per time-slot control space includes all possible sectorizations:

$$\begin{aligned} \mathbf{X}^{\text{BP}}(t) &:= \arg \max_{\mathbf{X} \in \bigcup_{\sigma \in \Gamma(\mathbf{K})} \mathcal{X}_{G^\sigma}} \{ \mathbf{D}^\top(t) \cdot \mathbf{X} \} \\ &= \arg \max_{\mathbf{M} \in \mathcal{M}_H^K} \{ \mathbf{D}^\top(t) \cdot \mathbf{M} \}. \end{aligned} \quad (28)$$

Here, $\mathbf{D}(t)$ denotes the vector of queue differentials (i.e., backpressure) at time t , $\Gamma(\mathbf{K})$ represents all possible sectorizations (each node n having K_n sectors), and \mathcal{X}_{G^σ} is the set of all feasible schedules *under a particular sectorization*. Equivalently, we can view $\bigcup_{\sigma \in \Gamma(\mathbf{K})} \mathcal{X}_{G^\sigma}$ as the set of all schedules that can be achieved by any valid sectorization choice, subject to the constraint that no node can activate more outgoing or incoming links than its allowed sector count. In the right-hand side of (28), \mathcal{M}_H^K denotes all *edge-activation vectors* \mathbf{M} (i.e., sets of simultaneously active edges) where each node n can activate at most K_n links total. Each such \mathbf{M} implicitly defines a feasible sectorization that permits those edges to be active simultaneously. Thus, we can choose an *edge set* first, then retroactively assign a sectorization to realize that edge set in practice. \mathcal{M}_H^K corresponds to the set of *b-matchings* [29] (for $\mathbf{b} := \mathbf{K}$): *each node may participate in at most b_n active edges*. The goal becomes selecting the subset of edges with the maximum total backpressure weight $\mathbf{D}^\top(t) \cdot \mathbf{M}$ under the node-degree constraints.

A natural way to represent the above optimization is through the following Integer Linear Program (ILP). We introduce binary variables $X_{nm} \in \{0, 1\}$ indicating whether the link (n, m) is active. Let $w_{nm} = \mathbf{D}_{nm}(t)$ be the backpressure weight for (n, m) . Then the per-slot optimization becomes:

$$\begin{aligned} &\max_{\{X_{nm}\}} \sum_{(n,m) \in \mathcal{L}} w_{nm} X_{nm} \\ &\text{subject to} \quad \sum_{m: (n,m) \in \mathcal{L}} X_{nm} \leq K_n, \quad \forall n \in \mathcal{N}, \\ &\quad X_{nm} \in \{0, 1\}, \quad \forall (n, m) \in \mathcal{L}. \end{aligned} \quad (29)$$

The constraint $\sum_m X_{nm} \leq K_n$ ensures that each node n cannot activate more links than its sector count, while the objective maximizes the total backpressure-weighted sum. In essence, (29) describes a *maximum weighted b-matching* in the graph of unsectorized nodes H . We refer the reader to [29] for a detailed discussion of b-matchings in combinatorial optimization. Solving (29) exactly in each slot

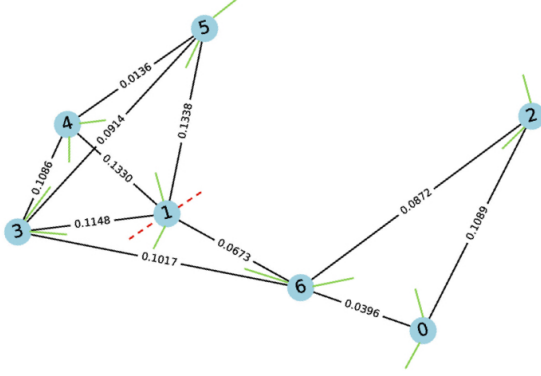


Fig. 6: An example 7-node network: the connectivity graph with the network flow \mathbf{f} labeled on each edge. The green lines indicate the node flow sectorization, $\pi(\mathbf{f})$, obtained via SECTORIZE- n with $K_n = 2, \forall n$ with a sectorization gain of 1.83. The red dashed lines indicate a “misconfigured” sectorization of node 1 in the bottleneck phenomenon.

provides a *throughput-optimal* dynamic sectorization policy. In practice, however, large-scale networks render per-slot exact solutions computationally prohibitive. Consequently, many systems could employ *approximation methods* (e.g., LP-based heuristics, iterative algorithms, or greedy selection) and/or *periodic re-sectorization* (solving the LP/Max-Weight at finite intervals [25]), preserving near-optimal throughput while substantially reducing overhead.

IX. EVALUATION

We now evaluate the sectorization gain and the performance of the distributed approximation algorithm via simulations. We focus on: (i) an example 7-node network, and (ii) random networks with varying number of nodes, number of sectors per node, and network flows. For each network and a given network flow, \mathbf{f} , we consider:

- $\pi_n(\mathbf{f}_n)$: the sectorization of node n returned by the distributed approximation algorithm, SECTORIZE- n (Algorithm 1 in Section VI-B), and $\pi(\mathbf{f}) = (\pi_n(\mathbf{f}_n) : \forall n \in \mathcal{N})$ is the sectorization of all nodes.
- $\mu^\pi(\mathbf{f})$ and $\mu^\varnothing(\mathbf{f})$: the approximate flow extension ratios for the sectorized and unsectorized networks, respectively (Section V).
- $g_\mu^\pi(\mathbf{f})$: the approximate sectorization gain achieved by $\pi(\mathbf{f})$ (Section V).

A. An Example 7-node Network

We consider a 7-node network, whose connectivity graph is shown in Fig. 6, with a network flow \mathbf{f} labeled on each edge and $\theta_{\text{th}} = 15.8^\circ$ (see Section III-B). For tractability and illustration purposes, we set $K_n = 2, \forall n$, and the green lines in Fig. 6 indicate the sectorization $\pi(\mathbf{f})$ returned by SECTORIZE- n . For this relatively small network, we can explicitly compute the flow extension ratios for both the sectorized network, $\lambda^\pi(\mathbf{f}) = \mu^\pi(\mathbf{f}) = 4.06$, and the unsectorized network, $\lambda^\varnothing(\mathbf{f}) = \mu^\varnothing(\mathbf{f}) = 2.22$. Therefore, the approximate sectorization gain $g_\mu^\pi(\mathbf{f})$ is equal to the explicit sectorization gain, i.e., $g_\mu^\pi(\mathbf{f}) = g_\lambda^\pi(\mathbf{f}) = 1.83$, which is close to $K_n = 2$.

Note that optimizing the sectorization of each node under a given \mathbf{f} is critical, since the misplacement of the sectoring axes of even a single node can largely affect the achievable sectorization gain. We call this effect the *bottleneck phenomenon* in sectorized networks, as illustrated by the following example. Considered the optimized sectorization $\pi(\mathbf{f})$ shown by the green lines in Fig. 6. If only the sectorization of node 1 is “misconfigured” to be the red dashed lines, the sectorization gain is decreased from 1.83 to 1.22. This is also intuitive since with this misconfiguration, all three edges incident to node 1 with the highest flows are served by the same sector.

Since nodes 1, 3, and 6 in Fig. 6 have a maximum node degree of 4, we also obtain a sectorization $\pi(\mathbf{f})$ by running SECTORIZE- n with $K_n = 4$. As expected, in the optimized sectorization for nodes 1, 3, and 6, one sectoring axis is put between every pair of adjacent edges. With this $\pi(\mathbf{f})$, we can also explicitly compute the flow extension ratios for the sectorized network $\lambda^\pi(\mathbf{f}) = \mu^\pi(\mathbf{f}) = 7.47$. This also confirms Remark 5.1 since the corresponding auxiliary graph G^π is bipartite under $\pi(\mathbf{f})$. With $\lambda^\varnothing(\mathbf{f}) = \mu^\varnothing(\mathbf{f}) = 2.22$, the sectorization gain is $g_\mu^\pi(\mathbf{f}) = g_\lambda^\pi(\mathbf{f}) = 3.36$. This example 7-node network demonstrates the performance and flexibility of SECTORIZE- n for optimizing the deployment and configuration of sectorized networks based on the network flows.

B. Random Networks

We now consider networks with randomly generated connectivity graphs, G . In particular, for each generated random geometric graph, N nodes are placed uniformly at random in a unit square area, and two nodes are joined by an edge if the distance between them is less than $2R$. We are interested in the effects of the following parameters of a random network on the sectorization gain:

- **Number of Nodes, N :** We consider random networks with different sizes of $N \in \{20, 40, 60, 80, 100\}$, and the network density increases with larger values of N .
- **Number of Sectors Per Node, K_n :** We assume all nodes have an equal number of sectors, $K_n = K, \forall n$, with $K \in \{2, 3, \dots, 15\}$.
- **Communication Range, $2R$:** With a given number nodes, N , the connectivity of the network can be tuned by the communication range between two nodes, $2R$. We consider $2R \in \{0.1, 0.2, \dots, 0.5\}$.
- **Uniformity of Network Flows, ϕ :** For a network flow \mathbf{f} , we define its *uniformity* by $\phi := \max_e f_e / \min_e f_e$, i.e., \mathbf{f} is more uniform if its ϕ is closer to 1. For a given value of ϕ , random network flows \mathbf{f} can be generated as follows. First, each element of $\mathbf{f}' = (f'_e)$ is independently drawn from a uniform distribution between $[1, \phi]$. Then, \mathbf{f} is set to be \mathbf{f}' after normalization, i.e., $\mathbf{f} = \mathbf{f}' / \|\mathbf{f}'\|$. We consider *Non-uniform*, *Uniform*, and *Very Uniform* network flows with $\phi = 1000, 10$, and 1.1 , respectively.

For random networks with a large number of nodes, we only consider $g_\mu^\pi(\mathbf{f})$ since it is computationally expensive to obtain $g_\lambda^\pi(\mathbf{f})$, which is the true sectorization gain achieved by $\pi(\mathbf{f})$. However, from Lemma 2, $g_\mu^\pi(\mathbf{f})$ provides good upper and lower bounds on $g_\lambda^\pi(\mathbf{f})$. The performance evaluation for each

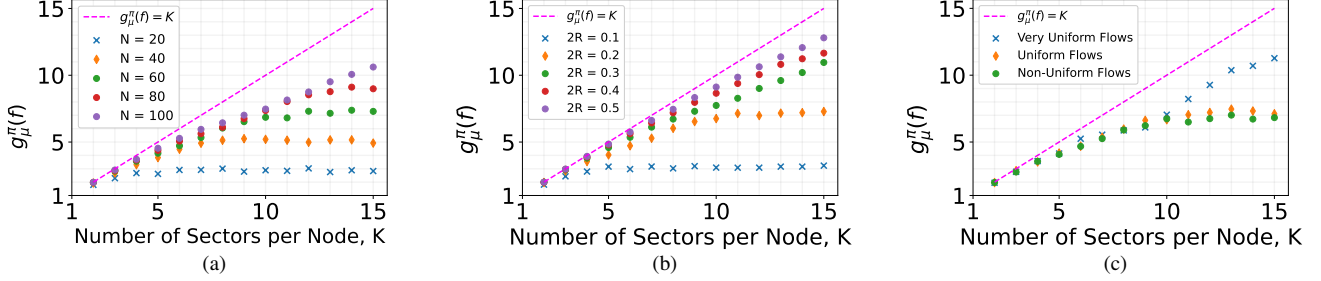


Fig. 7: The approximate sectorization gain, $g_{\mu}^{\pi}(\mathbf{f})$, as a function of the number of sectors per node, K , in random networks: (a) varying number of nodes $N \in \{20, 40, 60, 80, 100\}$ in networks with $2R = 0.2$ and *Uniform* flows, (b) varying communication range $2R \in \{0.1, 0.2, 0.3, 0.4, 0.5\}$ with *Uniform* flows and $N = 60$, and (c) varying network flows (*Non-uniform*, *Uniform*, *Very Uniform*) in networks with $N = 60$ and $2R = 0.2$.

point is based on 1,000 instances of the random networks and their corresponding $\pi(\mathbf{f})$ obtained by SECTORIZE- n .

Varying Number of Nodes, N . Fig. 7(a) plots the approximate sectorization gain, $g_{\mu}^{\pi}(\mathbf{f})$, as a function of the number of sectors per node, K , in a network with $2R = 0.2$ and uniform flows ($\phi = 10$), with varying number of nodes, N . Observe that $g_{\mu}^{\pi}(\mathbf{f})$ increases sublinearly with respect to K , and it approaches the identity line of $g_{\mu}^{\pi}(\mathbf{f}) = K$ as N increases, which is as expected. Note that with a practical value of K (e.g., $K \leq 6$), these networks can achieve $g_{\mu}^{\pi}(\mathbf{f})$ that is almost equal to the number of sectors per node, K . In addition, as the value of K increases, $g_{\mu}^{\pi}(\mathbf{f})$ deviates from K , which reveals a tradeoff point between the achievable sectorization gain ($g_{\mu}^{\pi}(\mathbf{f})$) and complexity of network deployments (N and K). In fact, for given parameters N , $2R$, and ϕ , i.e., for a given density of the network, there exists a number of sectors that saturates the gain $g_{\mu}^{\pi}(\mathbf{f})$. This is because after a sufficiently large number of sectors, the auxiliary graph of the network breaks down to isolated pairs of nodes. This fact also indicates that this phase transition phenomenon will also hold for the explicit extension ratio, $g_{\lambda}^{\pi}(\mathbf{f})$, since the graph is becoming eventually bipartite as we increase the number of sectors.

Varying Communication Range, $2R$. Fig. 7(b) plots the approximate sectorization gain, $g_{\mu}^{\pi}(\mathbf{f})$, as a function of the number of sectors per node, K , with $N = 60$, *Uniform* flows, $\phi = 10$, and varying communication ranges, $2R$. It can be observed that $g_{\mu}^{\pi}(\mathbf{f})$ increases sublinearly with respect to K . As expected, with the same number of nodes, $N = 60$, $g_{\mu}^{\pi}(\mathbf{f})$ is closer to K as the range increases. In fact, there is a relationship between the parameters N and $2R$: they both increase the number of neighbors for every node. The improved sectorization gains stem from the fact that since each node has a larger number of neighboring nodes (and thus links), a larger value of K and the optimized sectorization can support a larger number of concurrent flows.

Varying Uniformity of Network Flows, ϕ . Fig. 7(c) plots $g_{\mu}^{\pi}(\mathbf{f})$ as a function of the number of sectors per node, K , in a network with $N = 60$, $2R = 0.2$, and varying network flow uniformity (*Non-uniform*, *Uniform*, and *Very Uniform*). Overall, similar trends can be observed as those in Figs. 7(a) and 7(b). In general, more uniform network flows lead to

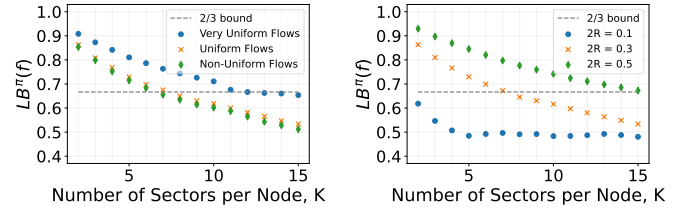


Fig. 8: The lower bound of approximation ratio of SECTORIZE- n , $LB^{\pi}(\mathbf{f})$ in (25), as a function of the number of sectors per node, K , with $N = 60$: (left) varying network flows in a network with $2R = 0.2$, and (right) varying communication ranges with *Uniform* flows.

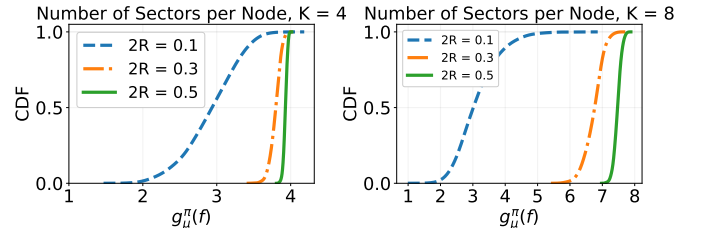


Fig. 9: The cumulative distribution function (CDF) of $g_{\mu}^{\pi}(\mathbf{f})$ with $N = 60$ and *Uniform* network flows.

improved values of $g_{\mu}^{\pi}(\mathbf{f})$, since non-uniform flows would have some larger flow components than the uniform ones, which on average increases the value of $\mu^{\sigma}(\mathbf{f})$ (see (10)). In addition, recall the bottleneck phenomenon described in Section IX-A, it is more beneficial to divide the flows of a node more equally across its sectors to achieve an improved sectorization gain.

Evaluation of the Lower Bound, $LB^{\pi}(\mathbf{f})$. Using simulations, we also evaluate the lower bound of the approximation ratio of SECTORIZE- n , $LB^{\pi}(\mathbf{f})$ in (25), which depends on $\mu^{\tilde{\sigma}}(\mathbf{f})$ and \mathbf{f} . Fig. 8 plots the value of $LB^{\pi}(\mathbf{f})$ as a function of K with varying uniformity of the network flows and node densities. It can be observed that for small values of K , $LB^{\pi}(\mathbf{f})$ is much higher than lower bound of $2/3$ provided by Theorem 6.2. In particular, the difference between the bounds increases dramatically and the approximation approaches the optimal for a small number of sectors. This is because in such networks, the maximum flow is expected to be small and hence $LB^{\pi}(\mathbf{f})$ can be improved when $\mu^{\tilde{\sigma}}(\mathbf{f})$ remains the same.

CDF of the Approximate Sectorization Gain, $g_{\mu}^{\pi}(\mathbf{f})$. Finally,

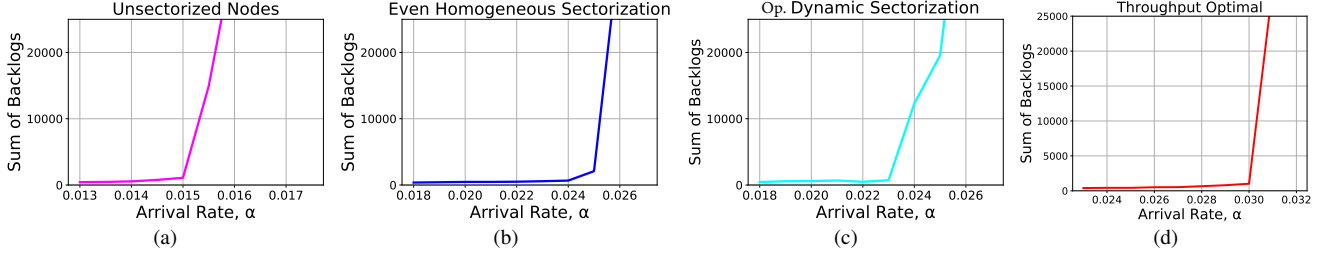


Fig. 10: The summation of the backlogs of a 16x16 grid network given a uniform traffic rate that is expressed with the scalar α for (a) unsectorized nodes, (b) Even Homogeneous Sectorization, (c) opportunistic dynamic sectorization, and, (d) throughput optimal routing

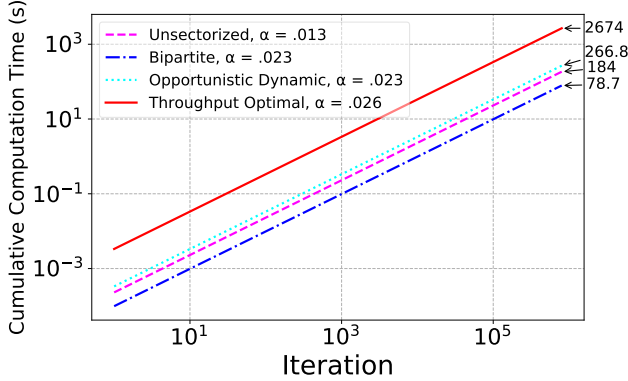


Fig. 11: Cumulative time needed (in seconds) for the calculation of the max-weight in every iteration of the backpressure algorithm.

we evaluate the relationship between $g_{\mu}^{\pi}(f)$ and the number of sectors, K . Fig. 9 plots the CDF of $g_{\mu}^{\pi}(f)$ with $N = 60$ and *Uniform* network flows with varying communication ranges. It can be seen that for networks with $2R = 0.3$, $g_{\mu}^{\pi}(f)$ has a median value of 3.7/6.5 for $K = 4/8$, respectively. This demonstrates the (sublinear) gain introduced by node sectorization, and this gain approaches the number of sectors per node, K , as the underlying is more connected.

C. Dynamic Routing: Sectorization and Induced Bipartiteness

In this subsection, we study the capacity and evaluate the behavior of backpressure in a regular grid network with $N = 16$ nodes and $K = 2$ for each node. In particular, we assume that the nodes are placed on a square grid and that every node has a range such that it can communicate with its four incident neighbors as well as with the four nodes on its diagonals.

We compare four sectorization techniques for the network: (i) unsectorized nodes, (ii) Even Homogeneous Sectorization, where each node is divided with a horizontal line creating north and south sectors, (iii) opportunistic dynamic sectorization as described in Section VIII-A, and, (iv) the throughput optimal dynamic sectorization described in Section VIII-B. In Even Homogeneous Sectorization, the network is divided using a simple horizontal line for each node, irrespective of the network state, effectively making the auxiliary graph bipartite (see Section VII). Conversely, dynamic sectorizations adapt to current flow conditions by sectorizing each node based on the ongoing network state, as detailed in Section VIII.

For the following numerical examples, we assume that the network receives uniform traffic and thus every pair of nodes

has a commodity that has an arrival rate of α . To implement that we assume that the packet arrival process $\{A_n^{(c)}(t)\}_t$ for every commodity c is a Bernoulli process with probability of success α . Nevertheless, we assume a dynamic setting where the network is not aware of the arrival rate matrix, α , and thus there is no information about the flow, f , that can be used when optimizing the node sectorization accordingly.

Capacity Increase. We assess the grid network’s capacity employing the four sectorization techniques mentioned earlier, under uniform traffic with an arrival rate of α . Specifically, we start from low values for the arrival rate α and increase until the backlogs “blow up”. This procedure is depicted in Fig. 10, where we plot the summation of the 16×16 different backlogs on the last iteration of the simulation with respect to the arrival rate. In Figs. 10(a) (*unsectorized network*), 10(b) (*Even Homogeneous Sectorization*), and 10(d) (*Throughput Optimal*) it can be observed that as the arrival rate exceeds the boundary of the capacity regions, the sum of the backlogs on the last iteration increases abruptly [26]. In Fig. 10(c) (*Opportunistic Dynamic Sectorization*), note that the capacity boundary does not emerge by a single “knee” point as is the case for the other three techniques. In the latter, for $\alpha \in [0.23, 0.25]$, though the network seems stable, requests accumulate in backlogs in a faster rate. The Even Homogeneous Sectorization’s performance closely aligns with that of the opportunistic dynamic sectorization, demonstrated by their capacity ratios to the unsectorized case, approximately $0.025/0.015 = 1.67$. The chosen Even Homogeneous Sectorization for this network is notably effective, as horizontal division fairly distributes uniform traffic across both sectors. In the case of the throughput optimal policy, we observe in Fig. 10(d) that the capacity is *two* times the one of the unsectorized network—which is the maximum we can expect using two sectors.

Bipartiteness & Speed-up. Next, we validate experimentally Theorem 7.3. In the previous section, we verified the capacity increase that the Even Homogeneous Sectorization introduce to the network. However, in Section VII, we proved that the auxiliary graph becomes bipartite, something that introduces speedup in the dynamic routing schemes. To validate this without using very sophisticated algorithms for the problem of maximum weighted matchings in bipartite graphs (e.g., [29]) we use Python’s NetworkX library [35]. This library provides a distinct function for identifying maximum weighted matchings in bipartite graphs, differing from the algorithm for non-bipartite graphs by generating a complete graph and addressing

the assignment problem instead. Despite not being as efficient as more recent algorithms, we observe an improvement in the network's dynamic routing performance using this method.

Specifically, in Fig. 11 we plot the cumulative time needed to calculate the max-weight up until a given time slot. That is, in a time slot t we plot the time the max-weight operations took cumulatively for time slots $1, 2, \dots, t$. For fairness, for every sectorization technique we set the network to receive arrival rate close to the boundary of the corresponding capacity region (see previous section). Therefore, the Even Homogeneous Sectorization case will be burdened with arrival rate that is 1.67 times greater than the unsectorized case. Nevertheless, note from the figure that with the Even Homogeneous Sectorization we decrease the time needed for the computations by a factor of 2.34 compared to the unsectorized case at time-slot 200,000. Essentially, in other words, although we increase the capacity region by a factor of approximately 1.67 and we make the connectivity graph more complex, we can decrease the time needed for the scheduling/routing operation by a factor of 2.34. The corresponding factors compared to the opportunistic dynamic sectorization is 3.39, and to the throughput optimal is 34. These ratios can be further increased with more sectors since, as proved, with sufficient distributed computing power, the more we sectorize the network, the more we decrease the time needed for its stabilization.

Fig. 11 also shows that the throughput optimal policy described in Section VIII-B needs significantly longer time to find the optimal sectorization and schedule compared to the opportunistic one (x10 times slower).

X. FUTURE DIRECTIONS

Analytical Trade-Offs and Choice of K . Our sectorization algorithm provides a provable approximation ratio and bounds but does not yield a closed-form relationship between the flow extension ratio and key parameters such as the number of nodes, network topology, flow properties, or the sector count K . Consequently, we do not offer explicit guidelines on how to select K in practice, aside from our numerical exploration in Figure 7, which suggests diminishing returns as K grows. Investigating a more rigorous, closed-form analysis of these parameter trade-offs is a natural avenue for future work and would be highly valuable for network designers.

Even Homogeneous Sectorization Guarantees. In Section VII, we showed how an Even Homogeneous Sectorization enforces a bipartite auxiliary graph, simplifying scheduling and speeding up backpressure stabilization. However, a more thorough characterization of its performance guarantees—especially when restricted to such sectorizations—would offer deeper insights.

Sectorizations to Alter Effective Topology. Finally, while we focus on even homogeneous sectorization in this work, other sectorization designs could be used to *embed* advantageous topological properties that benefit additional algorithmic tasks, such as graph coloring or clustering. By selectively adding (or removing) certain links from sectors, a sectorization can reconfigure the network's "effective" connectivity, potentially leading to improved performance for functions beyond scheduling

and routing. Investigating such systematic approaches—where the sectorization is chosen to induce a desired topology and/or properties—remains an intriguing future direction.

XI. CONCLUSION

In this paper, we considered wireless networks employing sectorized infrastructure nodes that form a multi-hop mesh network for data forwarding and routing. We presented a general sectorized node model and characterized the capacity region of these sectorized networks. We defined the flow extension ratio and sectorization gain of these networks, which quantitatively measure the performance gain introduced by node sectorization as a function of the network flow. We developed an efficient distributed algorithm that obtains the node sectorization with an approximation ratio of $2/3$. Further, we introduced a special class of sectorizations that boost the performance of dynamic routing schemes while increasing the capacity region. We also introduced a throughput-optimal scheme that jointly optimizes routing, scheduling, and sectorization for networks capable of adapting in real time. We evaluated the proposed algorithm and achieved sectorization gain in various network scenarios via extensive simulations.

REFERENCES

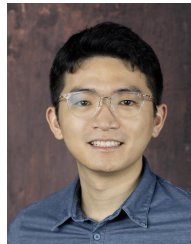
- [1] P. Promponas, T. Chen, and L. Tassiulas, "Optimizing sectorized wireless networks: Model, analysis, and algorithm," in *Proc. ACM MobiHoc'23*, 2023.
- [2] C. Shepard, H. Yu, N. Anand, E. Li, T. Marzetta, R. Yang, and L. Zhong, "Argos: Practical many-antenna base stations," in *Proc. ACM MobiCom'12*, 2012.
- [3] T. S. Rappaport, S. Sun, R. Mayzus, H. Zhao, Y. Azar, K. Wang, G. N. Wong, J. K. Schulz, M. Samimi, and F. Gutierrez, "Millimeter wave mobile communications for 5G cellular: It will work!," *IEEE Access*, vol. 1, pp. 335–349, 2013.
- [4] W. Saad, M. Bennis, and M. Chen, "A vision of 6G wireless systems: Applications, trends, technologies, and open research problems," *IEEE Network*, vol. 34, 2020.
- [5] M. Giordani, M. Polese, M. Mezzavilla, S. Rangan, and M. Zorzi, "Toward 6G networks: Use cases and technologies," *IEEE Commun. Mag.*, vol. 58, no. 3, 2020.
- [6] M. Agiwal, A. Roy, and N. Saxena, "Next generation 5G wireless networks: A comprehensive survey," *IEEE Commun. Surveys Tuts.*, vol. 18, no. 3, pp. 1617–1655, 2016.
- [7] "Facebook's 60-GHz Terragraph Technology," <https://spectrum.ieee.org/facebook-60ghz-terragraph-technology-moves-from-trials-to-commercial-gear>, 2019.
- [8] B. Sadhu, Y. Touse, J. Hallin, S. Sahl, S. K. Reynolds, Ö. Renström, K. Sjögren, O. Haapalahti, N. Mazar, B. Bokinge, *et al.*, "A 28-GHz 32-element TRX phased-array IC with concurrent dual-polarized operation and orthogonal phase and gain control for 5G communications," *IEEE J. Solid-State Circuits*, vol. 52, 2017.
- [9] Z. Gao, Z. Qi, and T. Chen, "Mambas: Maneuvering analog multi-user beamforming using an array of subarrays in mmWave networks," in *Proc. ACM MobiCom'24*, 2024.
- [10] T. Chen, P. Maddala, P. Skrimponis, J. Kolodziejski, A. Adhikari, H. Hu, Z. Gao, A. Paidimarri, A. Valdes-Garcia, M. Lee, *et al.*, "Open-access millimeter-wave software-defined radios in the PAWR COSMOS testbed: Design, deployment, and experimentation," *Computer Networks*, vol. 234, p. 109922, 2023.
- [11] M. Polese, M. Giordani, T. Zugno, A. Roy, S. Goyal, D. Castor, and M. Zorzi, "Integrated access and backhaul in 5G mmWave networks: Potential and challenges," *IEEE Commun. Mag.*, vol. 58, no. 3, pp. 62–68, 2020.
- [12] "SuperCell: Reaching new heights for wider connectivity," <https://engineering.fb.com/2020/12/03/connectivity/supercell-reaching-new-heights-for-wider-connectivity/>.
- [13] T. Korakis, G. Jakllari, and L. Tassiulas, "A MAC protocol for full exploitation of directional antennas in ad-hoc wireless networks," in *Proc. ACM MobiHoc'03*, 2003.

- [14] G. Zhang, Y. Xu, X. Wang, and M. Guizani, "Capacity of hybrid wireless networks with directional antenna and delay constraint," *IEEE Trans. Commun.*, vol. 58, no. 7, pp. 2097–2106, 2010.
- [15] Z. Yu, J. Teng, X. Bai, D. Xuan, and W. Jia, "Connected coverage in wireless networks with directional antennas," *ACM Trans. Sens. Netw.*, vol. 10, no. 3, 2014.
- [16] D. Zhang, M. Garude, and P. H. Pathak, "mmChoir: Exploiting joint transmissions for reliable 60 GHz mmWave WLANs," in *Proc. ACM MobiHoc'18*, 2018.
- [17] J. García-Rois, F. Gomez-Cuba, M. R. Akdeniz, F. J. Gonzalez-Castano, J. C. Burguillo, S. Rangan, and B. Lorenzo, "On the analysis of scheduling in dynamic duplex multihop mmWave cellular systems," *IEEE Trans. Wireless Commun.*, vol. 14, no. 11, pp. 6028–6042, 2015.
- [18] S. Roy, D. Saha, S. Bandyopadhyay, T. Ueda, and S. Tanaka, "A network-aware MAC and routing protocol for effective load balancing in ad hoc wireless networks with directional antenna," in *Proc. ACM MobiHoc'03*, 2003.
- [19] F. Dai and J. Wu, "Efficient broadcasting in ad hoc wireless networks using directional antennas," *IEEE Trans. Parallel Distrib. Syst.*, vol. 17, no. 4, pp. 335–347, 2006.
- [20] M. Gupta, A. Rao, E. Visotsky, A. Ghosh, and J. G. Andrews, "Learning link schedules in self-backhauled millimeter-wave cellular networks," *IEEE Trans. Wireless Commun.*, vol. 19, no. 12, pp. 8024–8038, 2020.
- [21] E. Arribas, A. F. Anta, D. R. Kowalski, V. Mancuso, M. A. Mosteiro, J. Widmer, and P. W. Wong, "Optimizing mmWave wireless backhaul scheduling," *IEEE Trans. Mobile Comput.*, vol. 19, no. 10, pp. 2409–2428, 2019.
- [22] T. Bai and R. W. Heath, "Coverage and rate analysis for millimeter-wave cellular networks," *IEEE Trans. Wireless Commun.*, vol. 14, no. 2, pp. 1100–1114, 2014.
- [23] D. Yuan, H.-Y. Lin, J. Widmer, and M. Hollick, "Optimal and approximation algorithms for joint routing and scheduling in millimeter-wave cellular networks," *IEEE/ACM Trans. Netw.*, vol. 28, no. 5, pp. 2188–2202, 2020.
- [24] P. Gupta and P. R. Kumar, "The capacity of wireless networks," *IEEE Trans. Inf. Theory*, vol. 46, no. 2, pp. 388–404, 2000.
- [25] L. Georgiadis, M. J. Neely, L. Tassiulas, *et al.*, "Resource allocation and cross-layer control in wireless networks," *Foundations and Trends® in Networking*, vol. 1, no. 1, pp. 1–144, 2006.
- [26] L. Tassiulas and A. Ephremides, "Stability properties of constrained queueing systems and scheduling policies for maximum throughput in multihop radio networks," in *Proc. IEEE CDC'90*, 1990.
- [27] J. Edmonds, "Maximum matching and a polyhedron with 0, 1-vertices," *J. Research of the National Bureau of Standards B*, vol. 69, no. 125–130, pp. 55–56, 1965.
- [28] J. Kahn, "Asymptotics of the chromatic index for multigraphs," *Journal of Combinatorial Theory, Series B*, vol. 68, no. 2, pp. 233–254, 1996.
- [29] A. Schrijver *et al.*, *Combinatorial optimization: Polyhedra and efficiency*, vol. 24. Springer, 2003.
- [30] J. Edmonds, "Paths, trees, and flowers," *Canadian J. Mathematics*, vol. 17, 1965.
- [31] B. Hajek and G. Sasaki, "Link scheduling in polynomial time," *IEEE Trans. Inf. Theory*, vol. 34, no. 5, pp. 910–917, 1988.
- [32] C. E. Shannon, "A theorem on coloring the lines of a network," *J. Mathematics and Physics*, vol. 28, no. 1–4, pp. 148–152, 1949.
- [33] C. Berge, "Graphs and hypergraphs," 1973.
- [34] M. Wattenhofer and R. Wattenhofer, "Distributed weighted matching," in *Proc. Int'l. Symp. Distributed Computing*, 2004.
- [35] A. Hagberg, P. Swart, and D. S. Chult, "Exploring network structure, dynamics, and function using networkx," tech. rep., Los Alamos National Lab, 2008.



working systems. He is also the recipient (co-author) of the Best Paper Award at the 12th IFIP WMNC 2019.

Panagiotis Promponas (Graduate Student Member, IEEE) received his Diploma in Electrical and Computer Engineering (ECE) from the National Technical University of Athens (NTUA), Greece, in 2019. He is currently a Ph.D. student in the Department of Electrical and Computer Engineering at Yale University. His primary scientific interests include resource allocation in constrained interdependent systems and the optimization of algorithms. Specifically, he focuses on the optimization and modeling of quantum networks and wireless net-



of-Things systems. He received the NSF CAREER Award, Google Research Scholars Award, IBM Academic Award, Facebook Fellowship, Wei Family Private Foundation Fellowship, Columbia Engineering Morton B. Friedman Memorial Prize for Excellence, Columbia University Eli Jury Award and Armstrong Memorial Award, the ACM SIGMOBILE Doctoral Dissertation Award Runner-Up, and the ACM CoNEXT'16 Best Paper Award.

Tingjun Chen (Member, IEEE) is an Assistant Professor of Electrical & Computer Engineering and Computer Science at Duke University. He received the B.Eng. degree in electronic engineering from Tsinghua University in 2014, the Ph.D. degree in electrical engineering from Columbia University in 2020, and was a Postdoctoral Associate with Yale University from 2020 to 2021. His research interests are in the area of networking and communications with a specific focus on next-generation wireless, mobile, and optical networks, as well as Internet-of-Things systems. He received the NSF CAREER Award, Google Research Scholars Award, IBM Academic Award, Facebook Fellowship, Wei Family Private Foundation Fellowship, Columbia Engineering Morton B. Friedman Memorial Prize for Excellence, Columbia University Eli Jury Award and Armstrong Memorial Award, the ACM SIGMOBILE Doctoral Dissertation Award Runner-Up, and the ACM CoNEXT'16 Best Paper Award.



systems and sensor networks. His most notable contributions include the max-weight scheduling algorithm and the back-pressure network control policy, opportunistic scheduling in wireless, the maximum lifetime approach for wireless network energy management, and the consideration of joint access control and antenna transmission management in multiple antenna wireless systems. Dr. Tassiulas is a Fellow of IEEE (2007) and of ACM (2020) as well as a member of Academia Europaea (2023). His research has been recognized by several awards including the IEEE Koji Kobayashi computer and communications award (2016), the ACM SIGMETRICS achievement award 2020, the inaugural INFOCOM 2007 Achievement Award "for fundamental contributions to resource allocation in communication networks", several best paper awards including the INFOCOM 1994, 2017 and Mobihoc 2016, a National Science Foundation (NSF) Research Initiation Award (1992), an NSF CAREER Award (1995), an Office of Naval Research Young Investigator Award (1997) and a Bodossaki Foundation award (1999). He holds a Ph.D. in Electrical Engineering from the University of Maryland, College Park (1991) and a Diploma of Electrical Engineering from Aristotle University of Thessaloniki, Greece. He has held faculty positions at Polytechnic University, New York, University of Maryland, College Park and University of Thessaly, Greece.

Leandros Tassiulas (Fellow, IEEE) is the John C. Malone Professor of Electrical Engineering at Yale University, where he served as the department head 2016–2022. His current research is on intelligent services and architectures at the edge of next generation networks including Internet of Things, sensing & actuation in terrestrial and non-terrestrial environments and quantum networks. He worked in the field of computer and communication networks with emphasis on fundamental mathematical models and algorithms of complex networks, wireless systems and sensor networks. His most notable contributions include the max-weight scheduling algorithm and the back-pressure network control policy, opportunistic scheduling in wireless, the maximum lifetime approach for wireless network energy management, and the consideration of joint access control and antenna transmission management in multiple antenna wireless systems. Dr. Tassiulas is a Fellow of IEEE (2007) and of ACM (2020) as well as a member of Academia Europaea (2023). His research has been recognized by several awards including the IEEE Koji Kobayashi computer and communications award (2016), the ACM SIGMETRICS achievement award 2020, the inaugural INFOCOM 2007 Achievement Award "for fundamental contributions to resource allocation in communication networks", several best paper awards including the INFOCOM 1994, 2017 and Mobihoc 2016, a National Science Foundation (NSF) Research Initiation Award (1992), an NSF CAREER Award (1995), an Office of Naval Research Young Investigator Award (1997) and a Bodossaki Foundation award (1999). He holds a Ph.D. in Electrical Engineering from the University of Maryland, College Park (1991) and a Diploma of Electrical Engineering from Aristotle University of Thessaloniki, Greece. He has held faculty positions at Polytechnic University, New York, University of Maryland, College Park and University of Thessaly, Greece.